Purification and kinetic characterization of glucose-6-phosphate dehydrogenase, 6-phosphogluconate dehydrogenase and soluble transhydrogenase of *Escherichia coli*

Diploma Thesis by Stefan Christen

Supervisors: Prof. U. Sauer, T. Fuhrer

Institute of Molecular Systems Biology, ETH Hönggerberg

February 2006 – August 2006

Contents

1 Summary

NADPH is the major reducing compound in anabolic reactions and through its catabolic production it directly couples anabolism and catabolism. This coupling can be overcome by the action of transhydrogenases that catalyze the hydride transfer between NAD(H) and NADP(H). Under aerobic batch conditions in *Escherichia coli* NADPH is mainly reduced by the pentose phosphate pathway, beside the membrane-bound transhydrogenase and the isocitrate dehydrogenase.

This thesis focuses on glucose-6-phosphate dehydrogenase and 6-phosphogluconate dehydrogenase, the oxidative enzymes of pentose phosphate pathway, to understand the kinetic properties and possible allosteric control of this pathway. After His_6-tag purification, kinetic parameters of both enzymes were determined by double-reciprocal and resulting secondary plots. Both enzymes were very sensitive to $NADP^+$ with K_m values of 23 µM and 9 µM for glucose-6-phosphate dehydrogenase and 6-phosphogluconate dehydrogenase, respectively. A screen was done with 20 metabolites to identify potential inhibitors of these enzymes. Glucose-6-phosphate dehydrogenase was inhibited by its products 6-phosphogluconate and NADPH. In contrast, 6-phosphogluconate dehydrogease was additionally affected by glycolytic compounds, from which fructose-1,6-bisphosphate had the highest impact. Its activity was also affected by compounds downstream the pentose phosphate pathway and by ATP.

Determined kinetic parameters were then used for modelling, where the $NADPH/NADP^+$ ratio turned out to be an important but not the only regulator of pentose phosphate pathway. Glucose-6-phosphate dehydrogenase was also influenced by substrate availability and 6-phosphogluconate dehydrogenase was affected by its product, ribulose-5-phosphate.

Further kinetic characterization in combination with the knowledge of *in vivo* metabolite concentrations will set a basis for dynamic modelling of central branching reactions in metabolism.

2 Introduction

2.1 NADPH metabolism in E. coli

NADPH is the major reducing equivalent in anabolic reactions, which serves in the generation of biomass. It is reduced in few reactions and biomass formation is the primary consumer of reduced cofactor with about 100 anabolic reactions (Fig. 2) [1]. Additionally, NADPH has a crucial role in the response to oxidative stress as an electron donor for enzymes such as glutathione reductase and alkyl hydroperoxidase [2, 3]. Under oxidative stress the transcription of glucose-6-phosphate dehydrogenase (Zwf), a member of the soxRS regulon, is induced.

To drive anabolic reactions, the NADPH/$NADP^+$ ratio is kept in a more reduced state than the NADH/NAD^+ ratio, the latter couple being important in the generation of ATP via oxidative phosphorylation. The current opinion about the relation between the oxidized and reduced pools is illustrated in Figure 1 [4-6].

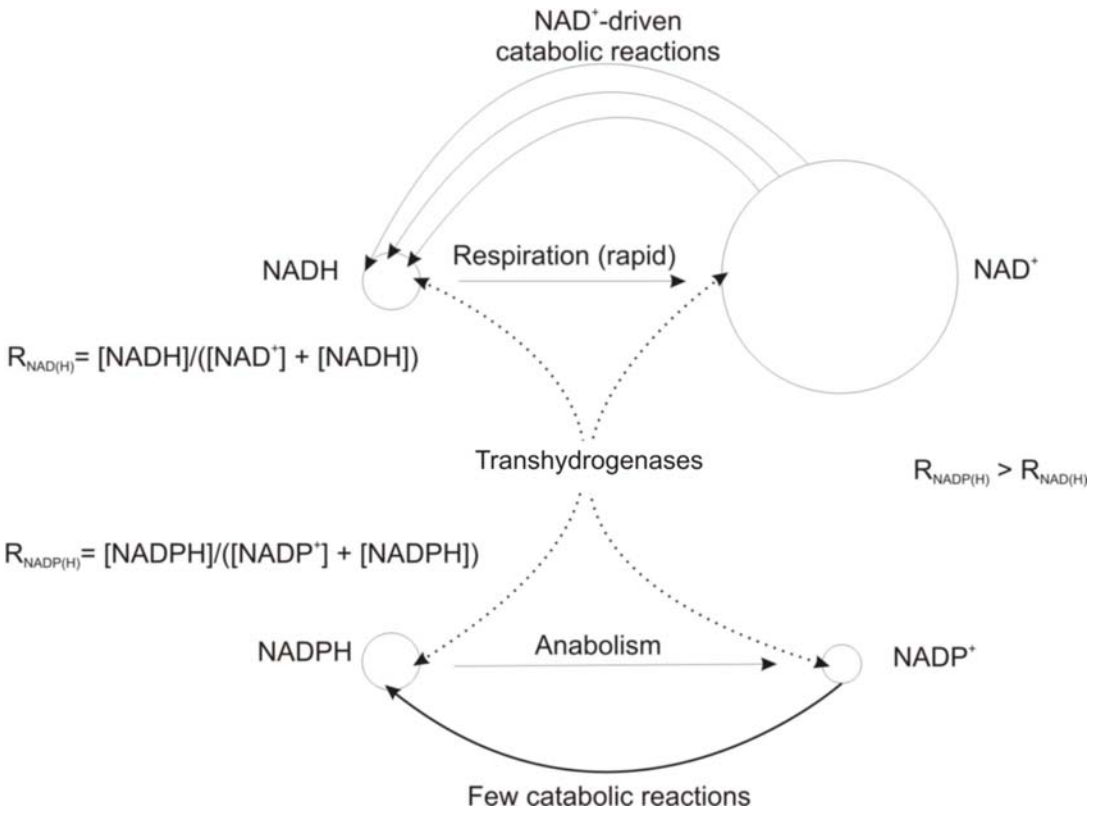

Figure 1: The current opinion about cofactor pools. The circles indicate the pool sizes [5][6]. NADH = 0.1 – 0.74 mM, NAD^+ = 1.47 – 1.69 mM, NADPH = 0.062 – 0.56 mM, $NADP^+$= 0.53 – 0.195 mM.

In metabolism, there are five important sites of $NADP^+$ reduction. These are the isocitrate dehydrogenase (Ict) in the TCA cycle, the oxidative branch of pentose phosphate (PP) pathway with glucose-6-phosphate dehydrogenase and 6-phosphogluconate dehydrogenase (Gnd), the membrane-bound pyridine nucleotide transhydrogenase (PntAB) and malic enzyme. All of these reactions with the exception of the membrane-bound transhydrogenase are located in central carbon metabolism, and lead therefore to a direct coupling of NADPH metabolism and central carbon metabolism (Fig. 2).

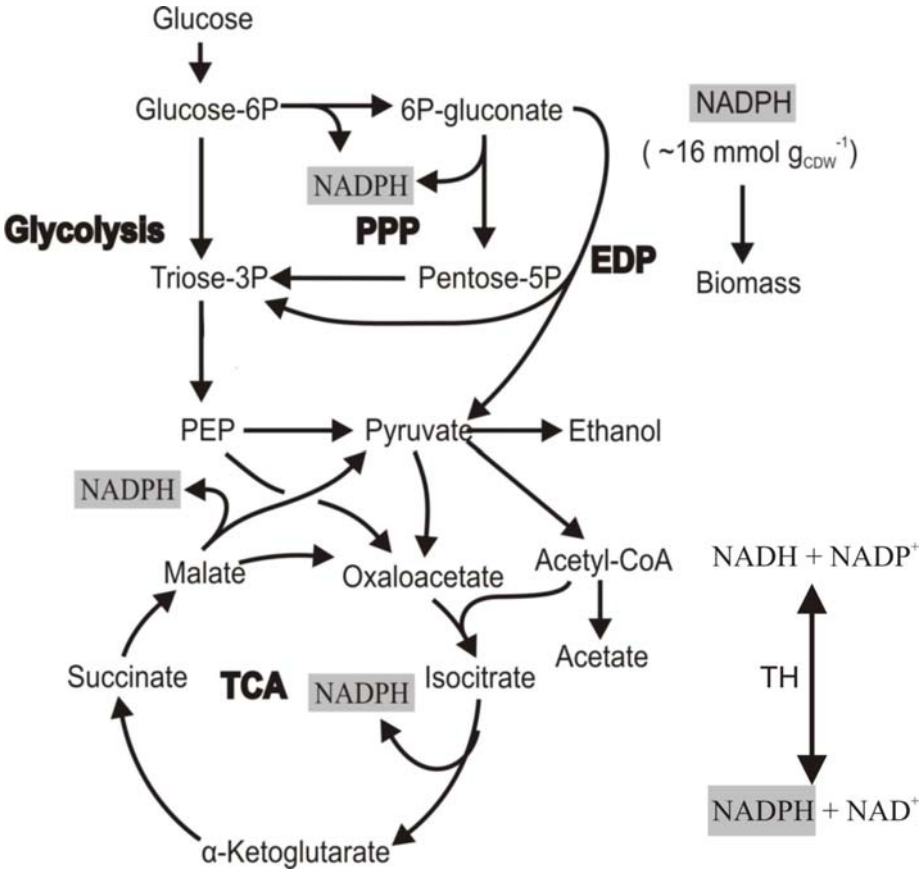

Figure 2: Metabolic network of *E. coli*. Abbreviations: PPP = Pentose phosphate pathway; EDP = Entner-Doudoroff pathway; TCA = citric acid cycle, TH = transhydrogenase.

^{13}C-labelling experiments revealed that under aerobic batch conditions on glucose, $NADP^+$ is reduced in *E. coli* to 35-45 % by the oxidative PP pathway, to 20-25 % by the Ict and to 35-45 % by the activity of PntAB [7]. In spite of the high relative flux through PP pathway in *E. coli* (25%), the NADPH production in catabolic reductions does not fulfil the demand for biomass production. This underproduction is overcome by the membrane-bound transhydrogenase PntAB. The activity of PntAB seems to be crucial to have an balanced

NADPH metabolism in *E. coli*, since the maximal growth rate decreases in PntA knockout mutants [7].

The question arises, if NADPH and $NADP^+$ have a key regulatory role in central carbon metabolism, since it is reported for several organisms, that it has high impact on the kinetic performance of enzymes [8-10]. In our case, the regulation at the branch point of glycolysis and pentose phosphate pathway by cofactors is of interest and that can be addressed by kinetic studies.

2.2 The role of transhydrogenases

Due to the fact that the generation of NADPH is coupled to catabolic reactions, there are several ways in microbia to overcome the potential imbalance of the NADPH production and consumption. Basically decoupling can be achieved by three ways. First, there are two isoforms of pyridine nucleotide transhydrogenases. One is membrane-bound and energy-dependent and relies on a proton-gradient over the inner membrane, whereas the other is soluble and energy-independent. Pyridine nucleotide transhydrogenases catalyze the hydride transfer between the phosphorylated and non-phosphorylated form (Fig. 3) [11, 12]:

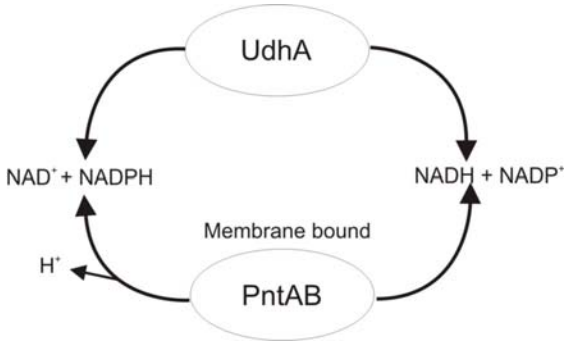

Figure 3: Transhydrogenase mechanism in *E. coli*. UdhA is the soluble energy-independent transhydrogenase, whereas PntAB is membrane bound and depends on a H^+- gradient. The direction of the reaction by PntAB is to the generation of NADPH, since it is driven by the proton gradient. UdhA, in contrast has more reversibility, but catalyzes rather the generation of NADH.

Through their action, certain redox ratios of either cofactor can potentially be maintained [11]. Most microbes contain only one isoform. Second, some organisms such as *E. coli* and *S. cervisiae* contain NAD^+ kinases that can directly convert NAD^+ to $NADP^+$ at the expense of ATP [13]. Third, combinations of reactions catalyzed by enzymes with different cofactor specificities can catalyze transhydrogenation-like reactions without

affecting the catabolic net fluxes. Such cycles are called redox cycles. Alternatively NADPH imbalance can be avoided through redistribution of fluxes and the use of NADPH-dependent isoenzymes.

In *E. coli,* both isoforms of transhydrogenases are found and as there is a underproduction of NADPH under aerobic growth on glucose. The role of PntAB is the reduction of $NADP^+$ to NADPH [7]. The physiological role of the second, energy-independent transhydrogenase in *E. coli* wild type (UdhA, EC 1.6.1.1) would be the balancing of an NADPH overproduction. This is the case when grown on acetate or in phosphoglucose isomerase (*pgi*) knockout mutants, where the carbon flux is forced through PP pathway, which leads to a NADPH overproduction [4, 10]. *udhA-pgi*-double knockout mutants have shown no growth on glucose, which could have been restored by plasmid-based expression of UdhA [14]. Another NADPH overproducing condition is given by growing the cells in glucose-limited chemostats, where 80% of the specific glucose uptake rate flows through the TCA cycle at a dilution rate of 0.4 h^{-1}, what leads to excessive reduction of $NADP^+$ through Ict [7, 15]. However, during aerobic growth on glucose, *E. coli* exhibits a NADPH underproduction and at the same time shows both PntAB and, surprisingly, UdhA activity in *in vitro* assays [1]. The first soluble transhydrogenase (Sth) was cloned in *P. fluorescens* and revealed that the enzyme is related to the family of flavoprotein disulfide oxidoreductases. The *sth* sequence of *P. fluorescens* was found to have 77% similarity and 60 % identity to the *E. coli udhA*. Both STHs have a threonine at the position of one of the redox-active cysteines which is characteristic for the family of flavoprotein disulfide oxidoreductases [16].

Enzyme	UdhA (EC 1.6.1.1)	
General Properties	▪ N-terminal region is suggested to have a dinucleotide binding domain. ▪ Molecular weight 51.5 ± 3.5 kDa. ▪ Suggested to be a homoheptamer or homoocatamer.	[16]

Table 1: properties of UdhA; no kinetic data are available yet.

Additionally soluble transhydrogenases have the potential for application in cell free systems in recycling of $NADP^+$ and NADH, as was shown with the transhydrogenase of *P.*

fluorescens in a process for the production of the opiate drug hydromorphone, which suffers from depletion of $NADP^+$ and NADH [17].

No kinetic studies on transhydrogenases are currently published. The question that arises is how UdhA is allosterically regulated and if its action maintains a certain cofactor ratio in *E. coli*. Another point that can be addressed by kinetic studies concerns the reversibility of the reaction catalyzed by the enzyme and if this leads to a role under conditions of aerobic batch growth on glucose.

2.3 Pentose phosphate pathway – glucose-6P dehydrogenase and 6-phosphogluconate dehydrogenase

The PP pathway synthesizes pentoses from hexoses or glycolytic intermediates, from which Ribose-5-phosphate is most important as it serves in the synthesis of ribonucleotides from which deoxyribonucleotides and nucleic acids subsequently can be formed. In addition, aromatic amino acids are synthesized from erythrose-4-phosphate, another metabolite present in the PP pathway. Another role of the PP pathway is the regeneration NADPH in the first and third reaction steps of the oxidative part of the pathway [18]. From metabolic flux experiments it is known that *E. coli* directs a relative carbon flux of ~25% through PP pathway on glucose minimal medium, which is high compared to other bacteria with the exception of *B. subtilis* [7, 19]. Additionally the flux through PP pathway seems to be rather stable, as was shown in knockout mutants of several global transcriptional regulators [20].

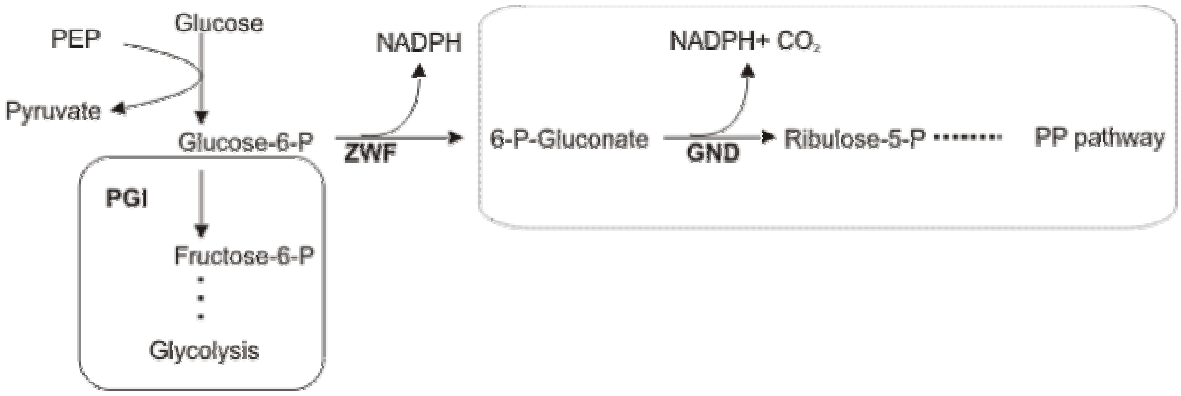

Figure 4: The branch point of Glycolysis and PP pathway. Zwf and Gnd catalyze the first reactions in the direction of PP pathway, while $NADP^+$ is reduced to NADPH.

To date, the regulation of routing catabolic fluxes into the PP pathway is not clear and a possible direct link to NADPH metabolism is discussed. In particular, the kinetic characteristics of both Zwf and Gnd are of interest, which would shed light on the relationship between cofactor redox state of the cell and PP pathway activity. The first reaction is the branch point of glycolysis and PP pathway (Fig 4). It is catalyzed by glucose-6-phosphate dehydrogenase (Zwf, EC 1.1.1.49). Glucose-6-phosphate is converted to 6-phosphogluconate, which is coupled to $NADP^+$ reduction. The K_m values for glucose-6-phosphate and $NADP^+$ in *E. coli*, determined in the 70ies, are 0.07-0.145 mM and 0.010-0.015 mM, respectively [9, 21, 22] . The enzyme is reported to be rather specific for its substrate with a 100 – fold higher K_m for NAD^+ than for $NADP^+$ and found to be inhibited by NADPH in an allosteric way (K_i = 0.01 mM). Additionally ATP, GTP, acetyl-CoA and coenzyme A did not exhibit an inhibitory effect. Sanwal also concluded that the oxidative PP pathway serves primarly to generate reducing power (NADPH) for the reductive need of the cell [9]. Other studies reveal that Zwf is involved in oxidative stress, since the level of Zwf increases by induction by the superoxide-generating agent paraquat and serves in generating NADPH. The regulation by oxidative stress takes place on the transcriptional level [23]. A summary of reported properties of Zwf is given in table 2.

Enzyme	Zwf (EC 1.1.1.49)	
General Properties	▪ Expression is increased by agents that endogenously generate superoxide (O_2^-) free radicals, as it is a member of the soxRS regulatory system. ▪ For many species it is reported to be a monomer, dimer or tetramer.	[3] [23] [24] [25]
Kinetic data reported from *E. coli*	▪ K_m(G6P) = 0.07 – 0.145 mM ▪ $K_m(NADP^+)$ = 0.01 – 0.015 mM ▪ K_i(NADPH) = 0.01 mM competitive for $NADP^+$ 0.04 mM Kic for G6P 0.18 mM Kiu for G6P ▪ No inhibition by ATP, AMP, ADP, GTP, acetyl-CoA and CoA, ribose-5-phosphate, phosphoenolpyruvate, fructose-1,6-bisphosphate, 3-phosphoglycerate ▪ No effect of NADH to concentrations of 0.3 – 0.5 mM	[21] [9] [22] [6]

Table 2: Properties of Zwf.

The third step from 6-phosphogluconate to ribulose-5-phosphate is catalyzed by 6-phosphogluconate dehydrogenase (Gnd, EC 1.1.1.44) (Fig. 4). It is a decarboxylating reaction, where $NADP^+$ is reduced to NADPH, which is thought to occur through at least three different steps: oxidation of 6PG at carbon 3, decarboxylation of the resultant 3-keto compound to an enediol, which in the third step tautomerizes to give Ribulose-5-phosphate. The decarboxylating step has been reported to be rate-limiting [26]. The *E. coli* enzyme is reported to be inhibited by several compounds of central carbon metabolism, like fructose-6-phosphate, fructose-1,6-bisphosphate, ribulose-5-phosphate, ADP and ATP [27].

Enzyme	Gnd (EC 1.1.1.44)	
General Properties	▪ Dimer (Monomer = 50 ± 1 kDa)	[28]
Kinetic data reported from *E. coli*	▪ K_m(6PG) = 0.01 – 0.1 mM ▪ $K_m(NADP^+)$ = 0.017 – 0.033 mM ▪ K_i = 0.049 mM competitive for $NADP^+$ ▪ Inhibition at concentrations of 1mM and 5mM ▪ F6P 0 % and 30 % ▪ FBP 63 % and 70 % ▪ Rib5P 18 % and 39 % ▪ PEP 6 % and 6 % ▪ ADP - and 70 % ▪ ATP 30 % and 100 %	[27] [28]

Table 3: Properties of Gnd

Studies on the regulation of Zwf and Gnd in *C. glutamicum* focussed on Zwf as the rate-controlling enzyme rather than Gnd. Experiments revealed that the *in vivo* activity of Zwf is primarily regulated by its specificity and by the concentration ratio $NADP^+$/NADPH. This leads to the hypothesis that oxidative PP pathway is in particular regulated by its main product, NADPH [10].

In the cases of Zwf and Gnd in *E. coli*, a complete screen over a big range of metabolites is still missing, what will reveal how the oxidative PP pathway is affected by these compounds Together with such a screen, reevaluation and determination of kinetics will

provide the basis for using available metabolite concentrations and finally investigate the regulation of oxidative PP pathway.

2.4 Enzyme Kinetics

Enzyme kinetics describes the kinetic mechanisms including potential allosteric regulation and different forms of inhibition. An enzyme can be kinetically characterized by several parameters. These are the rate of catalysis, V_0, which varies with the substrate concentration, the Michaelis constant K_M, which gives the substrate concentration at which V_0 equals ½ V_{max} and the turnover number k_{cat}. Additionally there are several types of enzyme inhibition through either products or other inhibitors which give a dissociation constant, K_i.

In practice, the initial rates of catalysis are determined at different substrate concentrations and plotted in a Lineweaver-Burk plot, which is a double reciprocal visualisation of the rate of catalysis against substrate concentration. From this plot the K_M and V_{max} under given conditions are determined [29].

2.4.1 Michaelis-Menten Kinetics

For one-substrate reactions, the rate of catalysis V_0, which is defined as the number of moles of product formed per second, varies with the substrate concentration. In order to neglect the backreaction, V_0 is determined in a time window where a small amount of product is generated, that is given directly after starting the reaction at the beginning of the steady-state phase. At fixed concentrations of enzyme V_0 is almost linearly proportional to [S], when [S] is small and nearly independent when [S] is large. In 1913, Leonor Michaelis and Maud Menten proposed a simple model to account for these kinetic characteristics.

Rate of formation of $ES = k_1[E][S]$

Rate of breakdown of $ES = (k_{-1} + k_2)[ES]$

Under steady state assumptions the concentrations of intermediates stay the same even if the concentrations of starting materials and products are changing. This finally leads to the Michaelis constant:

$$Km = \frac{k_{-1} + k_2}{k_1} = \frac{[E][S]}{[ES]} \qquad \text{(Eq. 1)}$$

K_m is an important characteristic of enzyme-substrate interactions and is independent of enzyme and substrate concentrations.

The concentration of free enzyme [E] is equal to the total enzyme concentration $[E]_T$ minus the concentration of the ES complex.

$$[ES] = [E]_T \frac{[S]}{[S] + Km} \quad \text{(Eq. 2)}$$

This leads to

$$V_0 = k_2[E]_T \frac{[S]}{[S] + Km} \text{ and } V_{\max} = k_2[E]_T \quad \text{(Eq. 3)}$$

Substituting results in the Michealis-Menten Equation:

$$V_0 = V_{\max} \frac{[S]}{[S] + Km} \quad \text{(Eq. 4)}$$

Through this equation it becomes clear that K_m is equal to the substrate concentration at which the reaction rate is at half of its maximal value [29].

2.4.2 Two Substrate Reactions

Zwf, Gnd and UdhA are considered as two-substrate reactions since the cofactors are treated as cosubstrates [5]. Mechanisms where both substrates have to bind before the product is formed are called *sequential*. The binding of the substrates can be *ordered* or *random*. A third mechanism, that is not further considered here, is the *ping-pong* mechanism where the product is released before the second substrates has bound.

For the determination of initial velocities at given concentrations in the forward reaction of sequential mechanisms the general description is given through:

$$V_0 = \frac{V_{\max}[A][B]}{K_{iA}K_{mB} + K_{mB}[A] + K_{mA}[B] + [A][B]} \quad \text{(Eq. 5)}$$

Where [A] and [B] are the substrate concentrations and K_{mA}, K_{mb} and K_{ia} are the Michaelis-Menten and dissociation constants.

If one of the two substrates is kept constant, the Michaelis-Menten equation can be simplified to its original form, and hyperbolic dependencies can be expected. Linearization methods as the Lineweaver-Burk plot can be applied:

$$\frac{1}{V_0} = \frac{K_{iA}K_{mB}}{V_{\max}[A][B]} + \frac{K_{mA}}{V_{\max}[A]} + \frac{K_{mB}}{V_{\max}[B]} + \frac{1}{V_{\max}} \quad \text{(Eq. 6)}$$

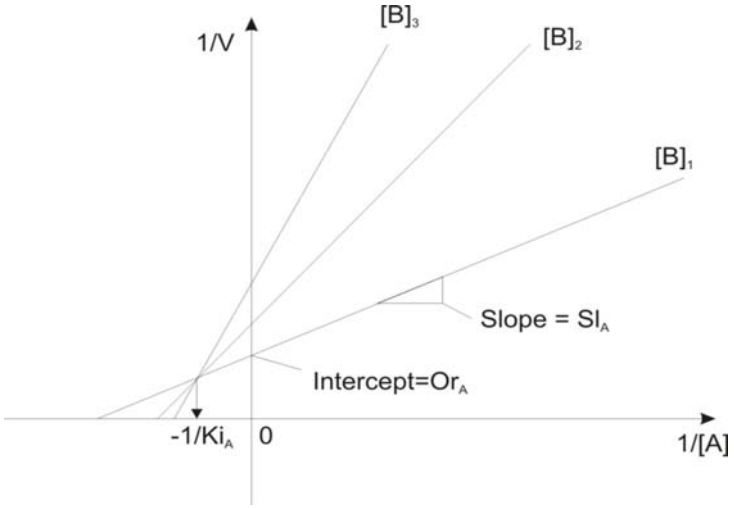

Figure 5: Lineweaver-Burk plot. [A] = concentrations of the first substrate added. $[B]_{1\text{-}3}$ = concnetrations of the second substrate. V = initial velocities. K_{iA} = dissociation constant of the first substrate.

The relative position of the intercept depends on the ratio of the constant and thus on the interactions of the two substrates. Without any interaction, i.e., for $K_{iA} = K_{mA}$ and $K_{iB} = K_{mB}$ the intercept is directly on the abscissa and has the value $-1/K_{mA}$ or $-1/K_{mB}$ if the cosubstrate is varied. For $K_{iA} < K_{mA}$ and $K_{iB} < K_{mB}$ the common intercept lies above the abscissa. For determination of the Michaelis and inhibition constants the secondary plot method was used. Linearity in these plots is an additional test for the assumed mechanism. The gradient Sl_A of the straight line in the primary plot is:

$$Sl_A = \frac{K_{iA} K_{mB}}{V_1 [B]} + \frac{Km_A}{V_1} \qquad \text{(Eq. 7)}$$

Plotting the gradient against 1/[B] gives a straight line with an abscissa intercept $-K_{mA}/K_{iA}K_{mB}$ (or $-1/K_{mB}$ for $K_{mA}=K_{iA}$). The ordinate intercepts Or_A of the primary plot

$$Or_A = \frac{Km_B}{V_1 [B]} + \frac{1}{V_1} \qquad \text{(Eq. 8)}$$

Primary plot		Secondary plot		Intercepts	
X axis	Y axis	X axis	Y axis	Ordinate	Abscissa
1/V	1/[A]	Sl_A	1/[B]	K_{mA}/V	$-K_{mA}/K_{iA}K_{mB}$
		Or_A	1/[B]	1/V	$-1/K_{mB}$
1/V	1/[B]	Sl_B	1/[A]	K_{mB}/V	$-1/K_{iA}$
		Or_B	1/[A]	1/V	$-1/K_{mA}$

Table 4: Calculation table for the determination of kinetic constants.

Alternative linearization methods are the Eadie-Hofstee plot and the Hanes plot [30].

2.4.3 Inhibition

Generally there are three types of reversible inhibition that affect the kinetic performance of an enzyme, *competitive, mixed (noncompetitive)*, and *uncompetitive* inhibition. All three types can be determined from Lineweaver-Burk plots (Figure 6).

In competitive inhibition the inhibitor competes with the substrate for the active site. This is based on a similar chemical structure of the inhibitor to the enzymes substrate. This results in an increasing value for K_m but does not affect V_{max}. The noncompetitive inhibitor binds to the enzyme – substrate complex as well as to the free enzyme and therefore a lower V_{max} is present, but K_m stays the same. In contrast, an uncompetive inhibitor binds to the enzyme – substrate complex what consequently affects both, Km and V_{max} [31].

$$\left(1+\frac{[I]}{K_i}\right) \qquad \text{(Eq. 9)}$$

This ends up in the general formula for non-competitive inhibition [30]:

$$V=\frac{V_{\max}[S]}{\left(1+\frac{[\mathrm{I}]}{\mathrm{K_{ic}}}\right)Km+\left(1+\frac{[\mathrm{I}]}{\mathrm{K_{iu}}}\right)[S]} \qquad \text{(Eq. 10)}$$

For competitive and uncompetitive inhibition the formulas are given in Equ. 11 and 12:

$$V = \frac{V_{max}[S]}{\left(1 + \frac{[I]}{K_{ic}}\right)Km + [S]} \qquad \text{(Eq. 11)}$$

$$V = \frac{V_{max}[S]}{Km + \left(1 + \frac{[I]}{K_{iu}}\right)[S]} \qquad \text{(Eq.12)}$$

Over secondary plots, where the reciprocal value of the slopes and ordinates is plotted against the inhibitor concentration, the abscissa determines the K_{iu} (ordinates) and K_{ic} (slopes) values.

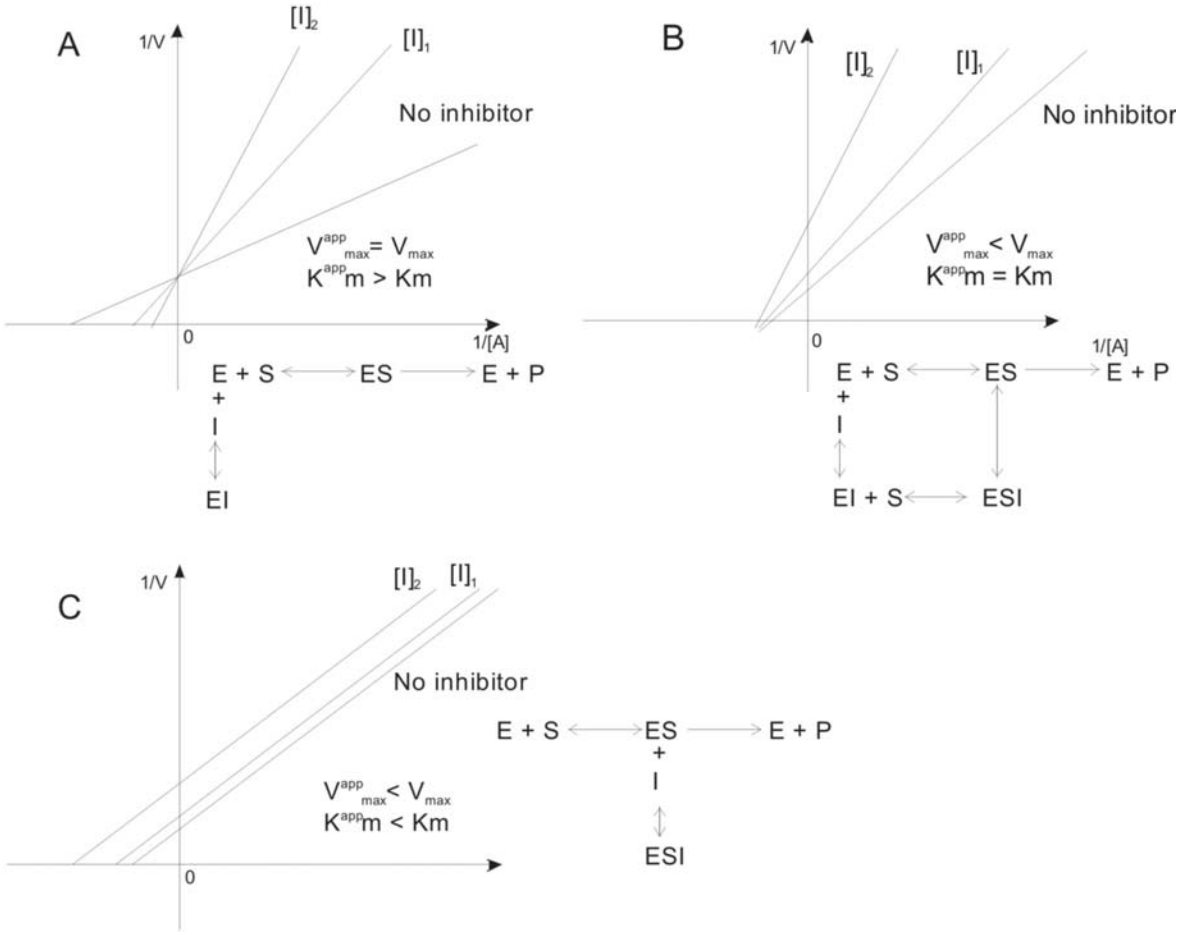

Figure 6: The different types of inhibition in a Lineweaver-Burk plot. One substrate is hold at an constant concentration, while the second substrate is varied with different fixed values of inhibitor. A: competitive inhibition, B: true non-competitive, C: uncompetitive inhibition. [I] = concentration of inhibitor, where the indices rise with increasing inhibitor concentration. E = Enzyme; S = Substrate, P = Product, app = apparent.

For two substrate reactions, one substrate is kept at a constant concentration, while the second substrate is varied at different inhibitor concentrations.

Equation 5 for noncompetitive inhibition will change as follows:

$$V_0 = \frac{V_{\max}[A][B]}{K_{iA}K_{mB}\left(1+\frac{[I]}{K_{icB}}\right)+K_{mB}[A]\left(1+\frac{[I]}{K_{icB}}\right)+K_{mA}[B]\left(1+\frac{[I]}{K_{icA}}\right)\left(1+\frac{[I]}{K_{iuB}}\right)+[A][B]\left(1+\frac{[I]}{K_{iuB}}\right)} \quad \text{(Equ. 13)}$$

Where the inhibitor is considered to inhibit competitively in respect to A and non-competitively with respect to B.

2.5 Goal of diploma thesis

This thesis focuses on the question whether or not allosteric regulation controls NADPH metabolism at the major conversion sites: PP pathway and the soluble transhydrogenase. Since Zwf and Gnd are directly involved in the branching between glycolysis and PP pathway, the kinetic regulation of these enzymes is of particular interest. Up to date the regulation of carbon routing into PP pathway is unclear and kinetic characterization of the enzymes involved provides the basis for further insights. In particular we focus on the question if this branch point is regulated by NADPH or possibly by other allosteric effectors. Therefore the proteins were purified and a screen over a wide range of metabolites was done. With the use of determined kinetic parameters the influence of the NADPH to $NADP^+$ ratio could be simulated.

The second focus is on the soluble transhydrogenase and its dependency on cofactor ratios or allosteric inhibition by other effectors under conditions with NADPH underproduction, where its activity was determined. Therefore we attempted to clone and purify UdhA of *E. coli*.

3 Material and Methods

3.1 Materials

3.1.1 Strains, primers, plasmids and enzymes

Strains

E. coli MG1655	Wild type K-12 strain $\lambda^- F^-$ rh-1
E. coli Dh5α	F^-, endA1, hsdR7 (rk^-mk^+), supE44, thi^-1, λ^-, recA1, gyrA96, relA1, φ80Δ*lacA*m15; Strain for plasmid amplification.
E. coli K-12, strain AG1 ▪ *zwf*-His_6 ▪ *gnd*-His_6	The strains were obtained from ASKA library [32] . The strains harbour the high copy number plasmid pCA24N , with an IPTG-inducible expression of the cloned ORF repression of expression by $lacI^q$ and an Histidine tag attached to the N-terminal end of ORF. The Plasmid carries a chloramphenicol resistance.

Plasmids

pTrc99a	High copy plasmid, Amp^R, strong trc promoter (IPTG inducible)
pbluescript SK(+)	High copy plasmid, Amp^R, MCS resides in the lacZ gene for β-galactosidase, which serves as reporter gene for the Blue/White screen. The transcription of the intact reporter gene is IPTG inducible.

Primers

The primers were designed with DNAstar and obtained from Microsynth.

Recognition sites for restriction are in *italic*, the restriction site itself is marked with a slash (/). The underlined region denotes the His_6 tag.

Eco_his_tag_upper (restriction by NcoI)	5'-GCA*C / C ATGG*GACATCATCATCATCATCATATGGGCCTGGGCCTGGTTAAGCAAGG-3'
Eco_his_tag_lower (restriction by HindIII)	5'-GCA*A / AGCTT*CTATTGGCCTGGTTTATCGTCCTG-3'
BamHI udhA	5'-CG*G/GATCC*GATGCCATAGTAATAGG-3'
HinDIII udhA	5'-CCC*A/AGCTT*TTTTAAAACAGGCGGTT-3'

Eco_udha_upper (restriction by NcoI)	5'-GCA*C / CATGG*GAATGGGCCTGGTTAAGCAAGG-3'
Eco_udha_lower (restriction by HindIII)	5'-GCA*A / AGCTT*CTATTGGCCTGGTTTATCGTCCTG-3'

udhA_op_BamHI	5'-AG*G / GATCC*AATAAAACGTCAGGGC-3'
udhA_op_HindIII	5'-CC*A / AGCTT*GGGGTTGTTTATCTGC-3'

Enzymes

Restriction enzymes	The restriction enzymes (Fermentas) were stored at -20°C.
T4 DNA Ligase	T4 DNA Ligase (New England Biolabs) was used with the appropriate 10x buffer. Ligase and 10x buffer were stored at -20 °C.
CIP Phosphatase	Obtained from NEB, stored at -20°C.
iProof ™ High-Fidelity DNA polymerase	Obtained from BioRad, stored at -20°C; yields blunt ended PCR fragments with an error rate of $4.4 * 10^{-7}$.
Phusion polymerase	Obtained from Finnzymes, stored at -20°C; yields blunt ended PCR fragments with an error rate of $4.4 * 10^{-7}$.

3.1.2 Chemicals

The used chemicals for the enzyme assays were purchased from Sigma, Fluka and Böhringer Mannheim.

3.1.3 Media and Buffers

3.1.3.1 Genetics

TAE buffer

242 g	Tris Base
57.1 ml	Glacial acetic acid
100 ml	0.5 M EDTA (pH 8)
	Dissolve in 1000ml ddH_2O.

Agarose Gel

0.4 g	Invitrogene Agarose
	Dissolve in 40 ml ddH_2O and boil until the Agarose has dissolved.
1 µl	EtBr solution

EtBr

1 g	EtBr
	Dissolve in 100 ml ddH_2O and store in the dark.

Colony lysis buffer

20 mM	TrisHCl (pH 8.3)
2 mM	EDTA
1 %	Triton X-100
	Store at 4°C.

3.1.3.2 Cultivation

LB Medium

5 g	Bacto tryptone
5 g	Bacto yeast extract
5 g	NaCl
	Were dissolved in 0.5 l ddH_2O.

For LB agar plates 10 g technical Agar were added.

Antibiotics

Ampicillin	For liquid medium 50 mg/ml
1000x (Amp)	For agar plates 100 mg/ml
	Solvent: ddH_2O
Chloramphenicol	20 mg/ml
1000x (Cmp)	Solvent: EtOH

Store aliquots at -20°C.

For agar plates: add antibiotic before pouring the plates, when the agar is around 40°C.

SOB medium

20 g	Bacto tryptone
5 g	Bacto yeast extract
0.5 g	NaCl
	Were dissolved in 1000 ml ddH_2O.

3.1.3.3 French press

French press buffer

3748 µl	100 mM TrisHCl pH 7.5, 5 mM $MgCl_2$
160 µl	25 X Proteaseinhibitor (Complete EDTA-free, Roche)
12 µl	1 M Dithiothreitol

Prepare fresh buffer before use.

3.1.3.4 Purification

Wash buffer (HisTrap)

20 mM	NaH_2PO_4
500 mM	NaCl
10 mM	Imidazole
15 mM	β-Mercaptoethanol

Adjust pH to 7.5

For on-column refolding prepare a gradient from 0-8 M Urea. Alternatively 6 M Guanidinium-HCl can be used.

Instead of β-Mercaptoethanol 5mM DTT can be used.

Elution buffer (HisTrap)

20 mM	NaH_2PO_4
500 mM	NaCl
X mM	Imidazole
15 mM	β-Mercaptoethanol

Prepare the elution buffer with X = 0.5 M and 0 M Imidazole and adjust pH to 7.5

Instead of β-Mercaptoethanol 5 mM DTT can be used.

Buffer for Dialysis

100 mM	TrisHCl
10 mM	$MgCl_2$
15 mM	β-Mercaptoethanol

Adjust pH to 7.5.

Instead of β-Mercaptoethanol 5 mM DTT can be used.

3.1.3.5 Solutions for determination of protein concentration

Biuret solution A

16 g	NaOH
	Dissolve in 100 ml ddH_2O.

Biuret solution B

1 g	$CuSO_4$ H_2O
6.7 g	KNa-Tartrat $4H_2O$
4 g	NaOH
2.5 g	KI
	Dissolve in 400 ml ddH_2O.

Bradford assay

For Bradford assay the 'Coomassie® Plus Protein Assay Reagent' from Pierce was used.

3.1.3.6 SDS-Gel

Running gel

2.85 ml	ddH_2O
1.5 ml	1 M Tris Base (pH 8.8)
1.5 ml	Acrylamide 40%
60 µl	SDS 10%
60 µl	Ammonium persulfate 10%
3 µl	TEMED

After pouring the running gel into the form, overlay it with Isopropanol to get rid of bubbles.

Stacking gel

2.88 ml	ddH_2O
0.75 ml	1 M Tris HCl (pH 6.8)
0.75 ml	Acrylamide 40%
40 µl	SDS 10%
40 µl	Ammonium persulfate 10%
4 µl	TEMED

Lämmli buffer (3x)

60 mM	TrisHCl (pH 6.8)
10 %	Glycerol
100 mM	DTT
2 %	SDS
0.005 %	Bromphenol blue
5 %	β-Mercaptoethanol

Running buffer

30.3 g	Tris Base
144.2 g	Glycine
10 g	SDS
	Dissolve in 10 l ddH2O.

Staining solution

2 g	Coomassie blue
75 ml	Glacial acetic acid
500 ml	EtOH
	Fill up to 1 l with ddH2O.

Destaining solution

800 ml	ddH2O
7.5 ml	Glacial acetic acid
100 ml	EtOH
	Fill up to 1 l with ddH2O.

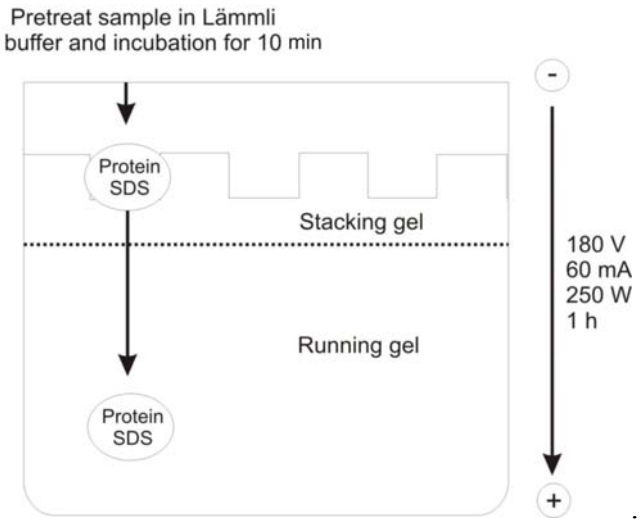

Figure 7: Scheme of a SDS protein gel

3.1.3.7 Buffers for enzyme kinetics

100 mM TrisHCl

10 mM $MgCl_2$

Adjust pH to 7.5

For measurements temperate it in a water bath at 29°C.

3.1.3.8 Metabolites

The different metabolites used in the screens, were aliquoted with a concentration of 0.1 M to 0.5 M and stored at -20°C

3.2 Methods

3.2.1 Cloning and Overexpression

3.2.1.1 Plasmid isolation

Promega Wizard Plus Minipreps DNA purification system was used with the protocol provided by the manufacturers.

3.2.1.2 EtOH precipitation and gel extraction

After digestion, the DNA fragments were precipitated with EtOH or loaded on a gel to remove false fragments and remaining restriction enzymes. For EtOH precipitation, the

digestion mix was dissolved in 2.5 volumes 100% ice cold EtOH and 0.1 volumes 3M Na-acetate. After 20 min incubation on ice, the solution was centrifuged for 15 min at 15000 rpm and 4°C. The supernatant was discarded and the pellet was air dried in order to remove the EtOH. Afterwards the pellet was dissolved in water. For gel extraction the QIAEX®II Gel Extraction Kit (150) from Qiagen was used.

3.2.1.3 Colony PCR

One colony from a LB agar plate was dissolved in 50 µl colony lysis buffer and spinned down briefly at 14000 rpm. After 15 min incubation at 95°C, cell debris was pelleted by centrifugation at 14000 rpm for 1min. 2 µl of the resulting supernatant were used for the PCR reaction.

ingredient	iProof DNA polymerase	Phusion DNA polymerase
Buffer	10 µl 5x HF-buffer	10 µl 5x HF-buffer
$MgCl_2$ (50 mM)	0.5 µl	-
Primer 1	1 µl	1 µl
Primer 2	1 µl	1 µl
Template	2 µl	2 µl
dNTP mix 10mM	1 µl	1 µl
ddH_2O	34 µl	34.5 µl
Polymerase	0.5 µl	0.5 µl

Table 5: Pipetting scheme of the used PCR reactions.

PCR reaction was started by incubating 2 min at 98°C, followed by 35 cycling steps beginning with 10 sec at 98 °C, annealing 30 sec at 50°C and 1min elongation at 72°C. Unfinished fragments were completed with 10 min at 72°C and the cycling was stopped by cooling down to 4°C.

3.2.1.4 Digestion and Ligation

Digestions always contained 10% of the appropriate buffer from Fermentas or NEB. The amount of enzyme was calculated for complete digestion in 1h at 37°C. The Digestion was carried out for 1-3 h at 37°C. For sequential digestions the first enzyme (HindIII) was heat inactivated for 25 min at 65°C. After Digestion, the fragments were purified by EtOH precipitation. Ligations were carried out over night at 4°C and over night at 16°C with 1:3

and 1:10 vector to insert ratios. 3 µl of the ligation mix was used for transformation by electroporation.

3.2.1.5 Electrocompetent cells and transformation by electroporation

A LB culture of cells was harvested at OD600 of ~1 by centrifugation at 5000 rpm for 15 min. The pellet was resuspended in 1 culture volume of ice cold water and centrifuged for 15 min at 5000 rpm. The resulting pellet was washed again with 0.5 volumes of ice cold water and centrifuged for 15 min at 5000 rpm. The last washing step included the resuspension in 0.1 volumes ice cold water and centrifugation for 15 min at 5000 rpm. The pellet was resuspended in 0.04 volumes 10% Glycerol and aliquots of 200 µl were stored at -20°C. 50 µl of cells were electroporated in a 1mm cuvette with 3 µl of ligation mix. Electroporator parameters were as follows 1.5 kV, 200 Ω and 25 µF. The time constants were controlled to be between 3.6 and 4.5. The cells were incubated for 1h at 37°C in SOB medium, centrifuged for 3min at 10000 rpm and streaked onto selection plates containing the appropriate antibiotics.

3.2.1.6 Dephosphorylation by CIP phosphatase

To prevent back ligation, the plasmid was dephosphorylated after gel extraction with CIP phosphatase. At first the plasmid was incubated 30 min at 56°C followed by 30 min at 37°C. Alkaline phosphatase removes 5' phosphate groups from DNA and RNA. It also removes phosphates from nucleotides and proteins. After dephosphorylation the fragment was purified with QIAquick PCR Purification Kit (50) from QIAGEN. Only the insert or the plasmid fragment was dephosphorylated so that the ligation could occur with one of the compatible sticky ends carrying phosphate groups.

3.2.1.7 Blue/White screen

The Bluescript SK(+) plasmid has the multiple cloning site in the *lacZ* gene, which encodes β-galactosidase. By inserting a fragment the gene is destroyed and the galactosidase reaction can not take place anymore. The transcription is IPTG inducible and as substrate the chromogenic X-gal can be used. Additionally the plasmid contains an ampicillin resistance.

For screening purpose, transformed cells were plate onto freshly prepared and dried LB agar containing 20 µl of X-gal (50 mg/ml), 30 µl IPTG (200 mM) and 50 µg/ml ampillicin.

After incubation over night, appearing blue colonies indicated religated plasmids and white colonies successful insertion respectively. The white clones were cultivated in LB liquid medium with ampicillin and after plasmid purification checked for right insertions on a agarose gel [33].

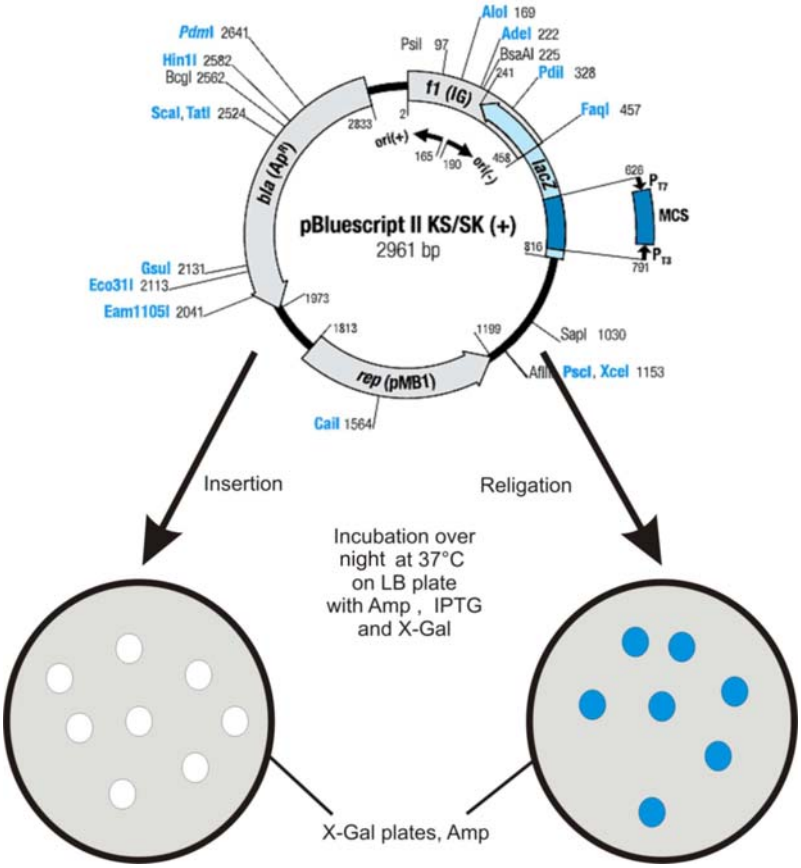

Figure 8: Method of Blue/White screen. Through the disruption of the reporter gene lacZ, β-Galctosidase cannot be expressed and this results in white colonies.

3.2.1.8 Overexpression

Overexpression was achieved by adding 25 µl of 200 mM IPTG to 50 ml cell culture. After growth over night, the culture was harvested and the purification of the enzyme could be started.

3.2.2 Purification

3.2.2.1 French Press

50 ml cell culture broth was harvested by centrifugation at 5000 rpm and 4°C for 15 min. The pellet was washed twice in 2ml 0.9% NaCl 10 mM $MgSO_4$. The pellet was then resuspended in 3.5 – 4 ml ice cold French press buffer and loaded into the French press mini cell from SIM AMINCO®, which was stored at 4°C. After 4 pressing steps with 1000 PSI the crude extract was centrifuged for 30 min at 15000 rpm and 4°C to get rid of cell debris.

3.2.2.2 Purification of His_6-tagged protein

In order to purify His_6-tagged proteins, 1ml HisTrap HP columns from Amersham Biosciences were used. The columns are prepacked with Ni Sepharose High Performance, which consists of 34 µM highly cross-linked agarose beads with an immobilized chelating group. The column has then been charged with Ni^{2+}-ions. Amino acids, like histidine, form complexes with Ni^{2+}.

All steps were conducted manually using a syringe what makes the method simple and fast. The 1 ml column was first washed with 5 ml ddH2O and equilibrated with 12 ml wash buffer. Afterwards 1.5 – 2 ml of centrifuged crude extract was loaded and the column was incubated for ~30 min at 4°C. The wash step was done with 12 ml wash buffer and then elution started. Elution was done with 4ml 100mM Imidazole, 8ml 300 mM Imidazole and 4 ml 500 mM Imidazole. 2 ml fractions were collected and loaded on a SDS gel to detect the positive samples for dialysis. For specific elution of the desired protein, the optimal imidazole concentrations were determined once using a imidazole gradient. In further purifications unspecific bound protein and the tagged protein were eluted directly using two specific imidazole concentrations. In the case of UdhA, for on-column refolding the wash step contained a gradient of 8 M to 0 M Urea or 6 M to 0 M Guanidine-HCl.

3.2.2.3 Dialysis

Dialysis was performed using Spectra/Por Float-A-Lyzer dialysis membranes from Spectrum Laboratories in order to get rid of high imidazole concentrations after elution from HisTrap. The membranes had an molecular weight cut off of 25 kDa and a volume of 5 ml, and were incubated 30 min in ddH_2O at 4°C before use. After loading the eluted

fractions the membrane was transferred into dialysis buffer and dialysed over night at 4°C. After dialysis the samples were ready to use for enzymatic assays. The membranes could be reused if they had been stored in 1% sodium benzoate.

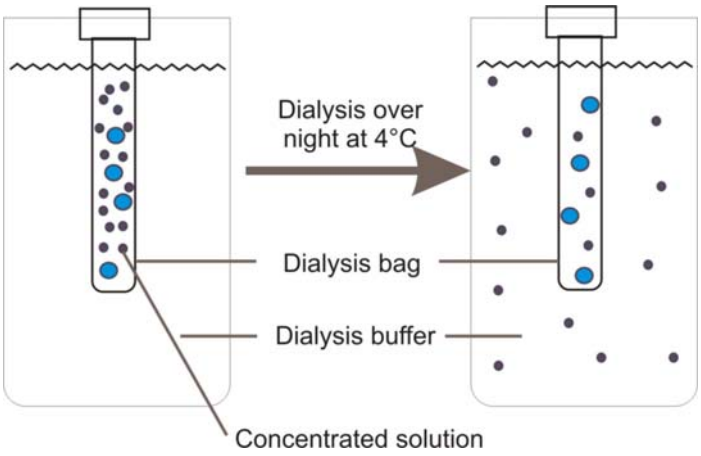

Figure 9: Dialysis.

3.2.2.4 Biuret and Bradford assay - estimation of protein concentration

For the determination of specific activities one has to know the enzyme concentrations. The method of the Biuret assay is based on the reaction of copper(II) with N atoms in the peptide bonds of proteins. Compounds containing peptide bonds give a characteristic purple colour when treated in alkaline solution with copper sulphate. There are relatively few substances that interfere with the biuret estimation like bile pigments, sucrose, tris, glycerol, ammonium ions and imidazole. Therefore the assay was not suitable to measure the concentration of protein after dialysis, because it still contained some imidazole.

For Biuret assay one has to dissolve 400 µl of the enzyme extract in 400 µl of biuret solution A. The sample was incubated 10 min at 95°C and then cooled down to room temperature. 1.2 ml of biuret solution B was added and the sample was incubated 30 min at 37°C and centrifuged for 20 min at 14000 rpm. OD 546 was measured and the enzyme concentration was determined.

Another assay that does not show high interference with imidazole is the Bradford assay. The Bradford dye assay is based on the equilibrium between three forms of Coomassie Blue G dye. Under strongly acidic conditions, the dye is most stable as a double-protonated red form. Upon binding to arginine and aromatic residues, it is most stable as an unprotonated, blue form.

1.5 ml ‘Coomassie® Plus Protein Assay Reagent’ from Pierce were pipetted into a 2 ml tube. 50 µl of protein sample were added and the sample was vortexed. Afterwards OD 595 was measured with a spectrometer.
For both assays a standard curve with bovin serum albumin was done.

3.2.3 Enzymatic assays

In practice several parameters have an impact on the kinetic performance of an enzyme. These are mainly ionic strength, temperature and pH. The potential disturbance of these parameters in enzymatic measurements require clearly defined assay conditions with constant pH, inonic strength and temperature[34].
The from the measurement resulting progress curve, where the absorption is plotted over time, has three phases which are a pre-steady-state, steady-state and equilibrium. The steady-state ranges from a few to several hundred seconds and it is used to determine the initial velocity V_0.
If one has to handle instable substances, one uses small aliquots from stock solutions which were hold in an ice bath. There should be a time window for the sample to equilibrate in temperature after mixing well and the cuvette holder of the photospectrometer has to be thermically controlled.
Metal ions are crucial with many enzymes, particularly with systems that require nucleotides. Changes in the ionic strength may also have an effect on enzyme performance. The concentration of free metal ions should not vary significantly with substrate concentration. There are two methods commonly used to achieve this. One is to maintain the total nucleotide concentration and metal concentration at a constant stoichiometric ratio or maintaining a constant excess of metal ion over the total nucleotide concentration. Additionally the performance of an enzyme is highly dependent on the pH, as the pH determines how the enzyme is charged. Therefore a buffer is usually used, which can hold a pH constant and all additives should have the same pH to ensure that the pH does not vary between the samples and during the assay itself. As the enzyme normally acts under physiological conditions, the pH was chosen at a physiological value of 7.5 ± 0.05.
Substrates were stored at -20°C and melted on ice, since they are highly unstable at room temperature. The same was done with potential inhibitors.
In our measurements the Spectramax Plus spectrometer from Molecular Devices was used, with a controlled temperature of 29°C and two second intervals single measurements. The

assay had a total volume of 1 ml with a total amount of additives of ~100 µl. The cuvettes were obtained from Greiner bio-one. OD 340 was measured over 1.5 min. For NADH and NADPH as additives a new reference was done, since they highly absorb at 340 nm (ε = 6.22 mM cm^{-1}). To obtain a good mixture, the cuvette was vortexed before measuring and when the second substrate was added, the cuvette was inverted. This led to a time window of 10 seconds, where no measurement could be done. For measurements with NADPH and NADH the vortexing was substituted by a inverting step, since otherwise the background was not stable.

The measured progess curve was regressed with a second order polynom to determine the initial velocity at the time point when the second substrate was added and the sample was mixed. Polynomes of higher degree were not suitable for regression because they were influenced by small fluctuations in the measurements. The whole workflow is summarized in Figure 10.

In order to screen for potential inhibitors the substrate concentrations were hold in the range of reported Km values. The concentrations of potential inhibitors were hold at 0.5-5 mM based on reported data [35].

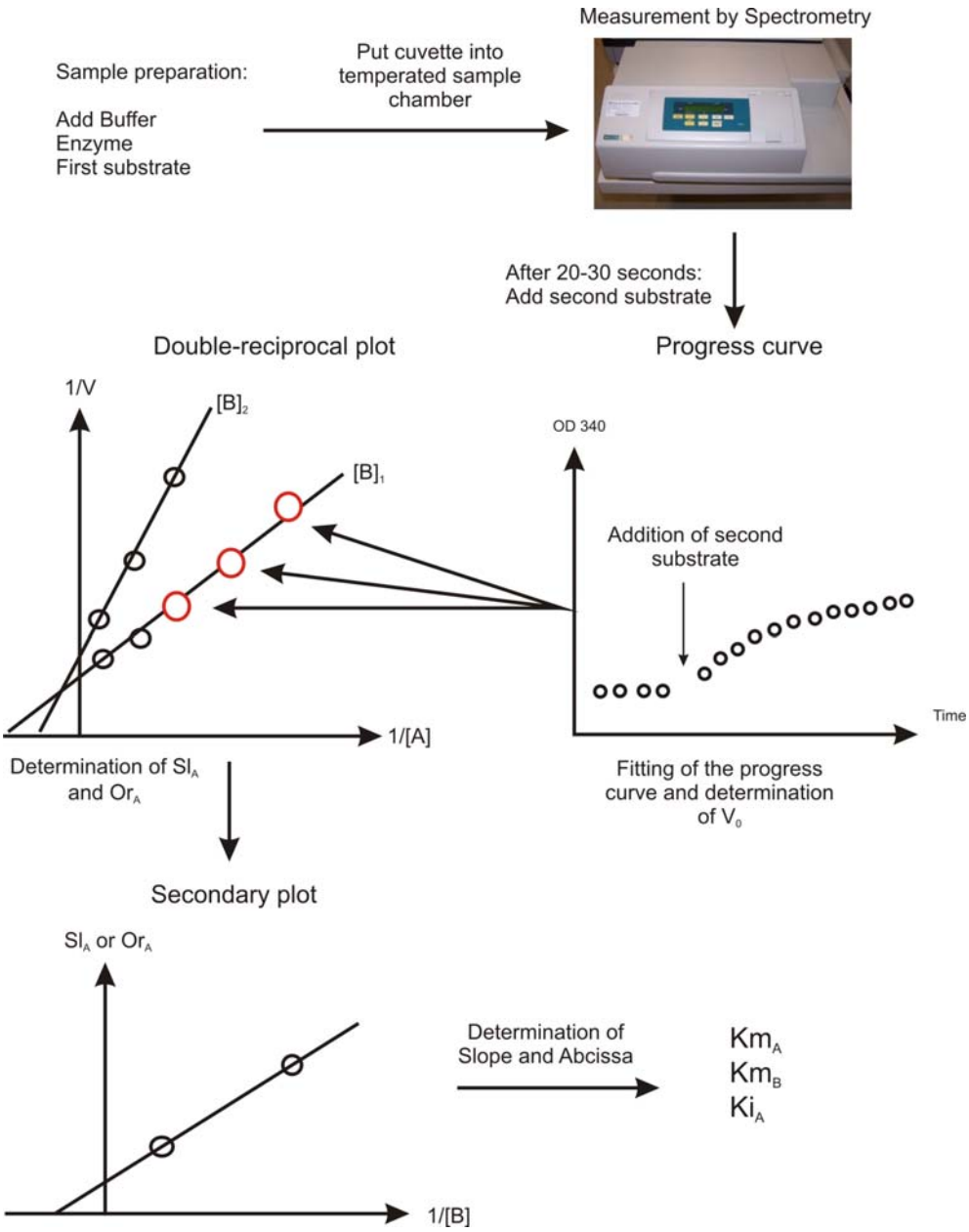

Figure 10: Workflow of enzymatic measurements. The measured absorbances directly end up in progressed curves which can be used for determination of the initial velocities. In a double reciprocal plot (e.g. Lineweaver-Burk plot) this velocities end up in a concentration dependent linearity. From these lines a secondary plot can be done from which the different K values can be determined.

4 Results

4.1 UdhA

4.1.1 His_6-tagged Protein

UdhA-His_6 was successfully cloned into the high-copy plasmid pTrc99A and transformed into *E. coli* Dh5α. The insertion was verified on an agarose gel, after cutting the plasmid with HindIII, which resulted in a single band at ~4.5 kb (Figure 11 A). The positive clones were sequenced by Microsynth. Since *E. coli* Dh5α was not suitable for overexpression due to low growth rates after induction with IPTG, the plasmid was purified and transformed into an *E. coli* Mg1655 wild type strain. After overexpression with 0.1 mM IPTG the resulting crude extract did not show a significant increase in activity. SDS gel electrophoresis of the crude extract and the centrifuged crude extract revealed formation of inclusion bodies (Fig. 11 B).

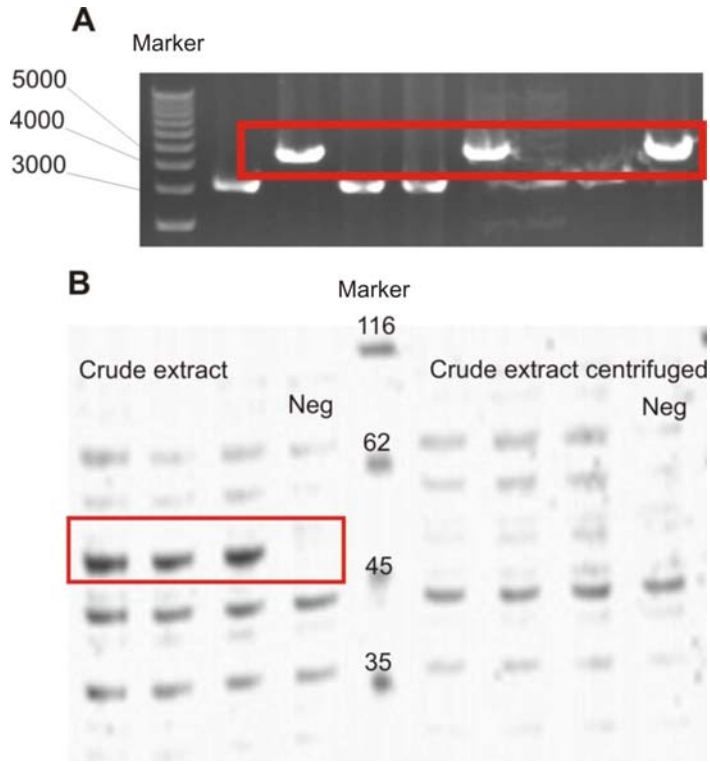

Figure 11: A: Verification of insertion after transformation. The gel indicates positive clones which carry the His_6-tagged UdhA (framed) with a band at ~4.5 kb. B: The SDS protein gel shows that the protein was overexpressed (framed) but has disappeared after centrifugation (right side), implying that the protein aggregated in the form of inclusion bodies. Neg is the negative control which does not show any band.

On-column-renaturation did not work, since the enzyme is reported to fold into multimeric form. Since every subunit carries the His_6-tag, they are separated on column and the multimerisation cannot take place. So it was decided to renaturate the enzyme by rapid dilution after the purification of the denaturated His_6-tagged protein. The SDS gel of the collected fractions indicated that the purification worked, since there was only one band detected at imidazole concentrations of 100 – 400 mM Imidazole. Rapid dilution at different dilutions of the recombinant enzyme and variable pH values resulted in no measureable activity of the protein (data not shown).

4.1.2 Overexpression of untagged from pTrc99a

Since His_6-tagged protein renaturation did not work, we decided to overexpress the protein without a His_6-tag and purify it by affinity chromatography. Several trials of inserting the PCR-amplified fragment into the vector ended up in religation of the vector as was seen on an agarose gel (data not shown). Despite several attempts and the use of different restriction enzymes in different combinations (HindIII, BamHI and NcoI) and different ratios of fragment to plasmid (ranging from 1:1 to 10:1) no successful products were obtained.

4.1.3 Insertion of the *udhA* gene into pbluescriptII SK(+)

As an alternative we used the pBluescriptII SK(+) vector. The vector has the advantage that a blue/white screen can be performed on plates, revealing clones with an insert by the colour of the colonies. As a test that digestion and ligation works, the fragment used before was successfully cloned into pBluescriptII SK(+) (data not shown).

Since overexpression is not inducible using pBluescriptII SK(+), new primers were used which carried the -35 and the -10 region of *udha*. The high copy number of the plasmid expected to yield a high UdhA expression. The new insert carried the same distinct restriction sites as the one used before (BamHI and HindIII). However, several trials with different conditions in the ligation ended up in religation of the plasmid as all colonies grown on a LB agar plate with X-Gal, IPTG and Amp were blue, what indicated that digestion was not successful. In order to get rid of religation the plasmid was dephosphorylated with CIP phosphatase, which resulted in no growth after ligation and transformation.

4.2 Zwf

4.2.1 Purification of His_6-tagged Protein

The strain from ASKA library was cultivated with three different concentrations of IPTG (0, 0.1 and 1 mM) [32]. After harvesting by centrifugation and cell breakage by French press, the resulting crude extract was centrifuged and the pellet solubilisized by Urea. The results clearly show that an induction with 0.1 mM IPTG is strong enough for overexpression and that no inclusion bodies had formed. The light bands that can be seen in the pellet fractions most probably derive from rest contamination by the supernatant (Fig 12 A). After column (HisTrap HP) operation of the supernatant, the enzyme was eluted with Imidazole concentrations of 200 to 300 mM. The gel indicates high purity of the enzyme, since only one single band can be seen (Fig 12 B).

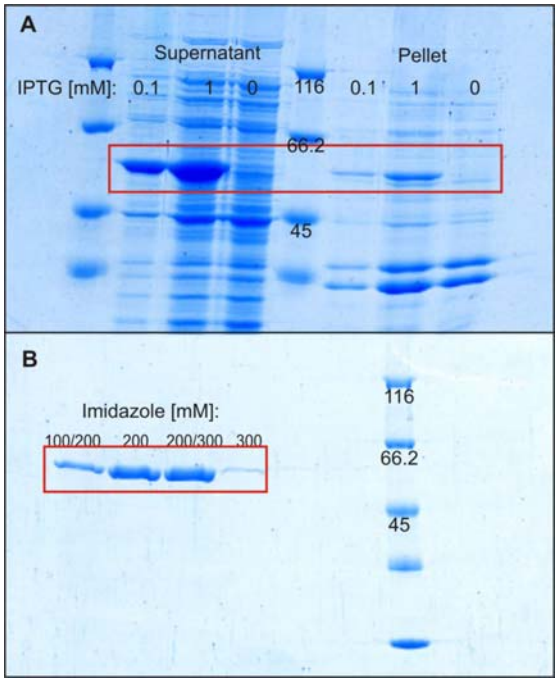

Figure 12: A: SDS gel after harvesting an overnight broth culture where overexpression was induced by different concentrations of IPTG. The fractions were loaded after centrifugation. It is shown, that induction by 0.1 mM and 1 mM IPTG leads to a strong overexpression and that no inclusion bodies are present in the pellet (framed). B: Elution profile after HisTrap. The enzyme could be eluted at Imidazole concentrations of 200 mM. Absence of bands indicates high purity of the enzyme (framed).

The positive fractions were dialysed over night to dilute the Imidazole from ~200 mM to ~1.5 mM. Bradford assay was done to determine enzyme concentration. The crude extract

had an specific activity of about 15000 U/g and the dialysate 187000 U/g. Units were defined as μmol L^{-1} min^{-1} (Fig. 13).

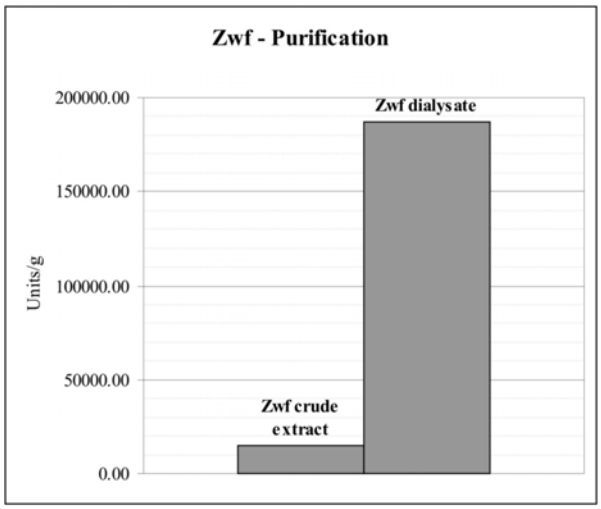

Figure 13: Purification of Zwf and evaluation of specific activity.

The total enzyme concentration decreased from 3.27 mg/ml to 0.172 mg/ml. The dialysate was directly used for further measurements without further purification steps.

4.2.2 Determination of K_m

K_m values were estimated with 20 μl of 8-10-fold diluted dialysate. The measurements resulted after regression with a second order polynome in initial velocities, which were plotted in a Lineweaver-Burk-plot, what resulted in straight lines with a common intercept (Fig.14 A). The Glucose-6-phosphate concentrations were varied from 50 μM to 400 μM, while the $NADP^+$ concentrations were between 20 μM and 150 μM. The linearity in the secondary plots supports that it is a sequential mechanism according to which the enzyme works (Fig 14 B). Over the equations in table 4, K_m values were determined. This resulted in a K_{mNADP+} of 23 μM and for G6P 136 μM. The dissociation constant K_{iNADP+} was 90 μM.

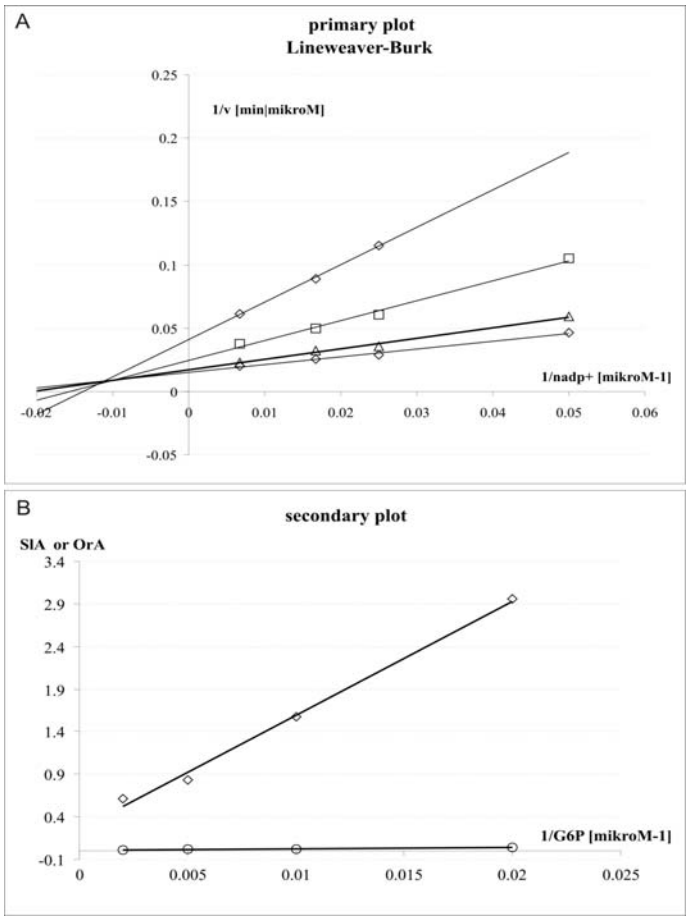

Figure 14: A: Lineweaver-Burk plot: The different concentrations of Glucose-6-phosphate were ◊ = 50 µM □ = 100 µM Δ = 200 µM ○ = 500 µM . B: secondary plots: ○ = Or_A ◊ = Sl_A from the ordinate and abscissa of these plotes the constants were directly determined.

4.2.3 Inhibitor screen

The inhibitor screen was performed with 20 µl of 8 fold diluted enzyme. In a fist screen the concentrations of $NADP^+$ and of Glucose-6-phosphate were chosen near the according K_m-values, so that inhibition would have been seen in a progressive curve and respectively in the resulting initial velocities. The concentrations of potential inhibitors were chosen to be close to physiological values ([35], supplement 2). Stocks were done in assay buffer or water and stored at -20°C. The potential inhibitors were thawed on ice and tested for influence on the pH not more than 0.1 pH units. Especially for organic acids like citrate and oxaloacetate the pH had to be adjusted with 5 M KOH and 6 M HCl. Additionally, the behaviour of the enzyme in 100 mM Tris HCl and 10 mM $MgCl_2$ was tested in a pH range from 6.7 to 7.7 units. The pH does not influence the acitivity of the enzyme in a range from 7 to 7.5 pH units (Fig. 15) and since the addition of different metabolites did only show a pH variability within that range, a potential effect on pH can be neglected.

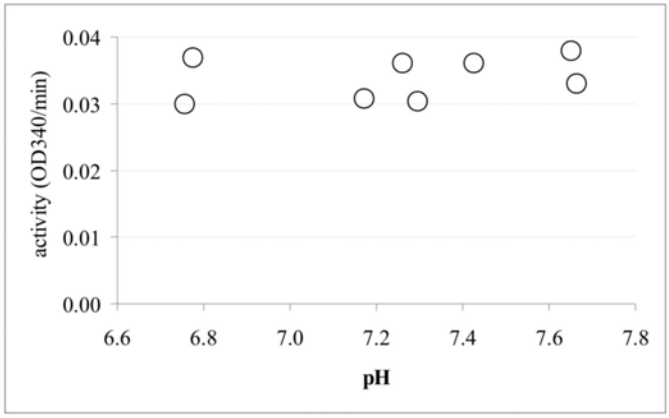

Figure 15: The dependency of Zwf activity from pH in a range of 6.8 to 7.6

Glycolytic compounds did not show an effect on the performance of Zwf as can be seen in Figure 16. Also the different compounds of the TCA cycle did not exhibit an influence on the activity with a glucose-6-phosphate concentration of 0.125 mM, except citrate at a concentration of 5 mM has reduced the activity of the enzyme over 20 %. Upon raising the concentration of glucose-6-phosphate to 0.3 mM in a second measurement, which will is closer to intracellular concentration, however, the effect was not present any more.

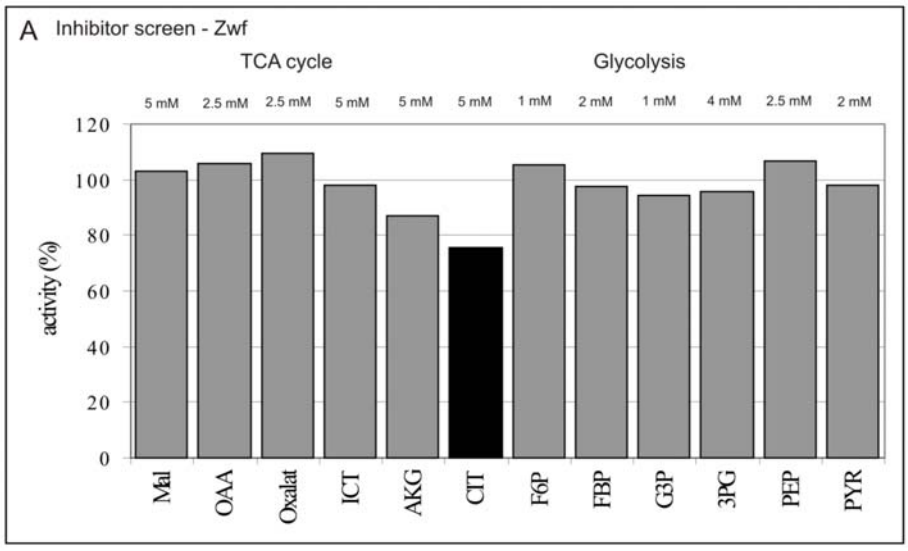

Figure 16: Inhibitor screen from intermediates of TCA cycle and glycolysis. [$NADP^+$] was 25 µM and [G6P] 125 µM. The concentrations above the bars indicate the chosen inhibitor concentration. Citrate (black) was the only compound which affected the activity of the enzyme.

Similarly, PP pathway intermediates did not show an inhibitory effect on the enzyme's activity at a Glucose-6-phosphate concentration of 0.3 mM, with the exception of 6-

phosphogluconate as the product of Zwf reaction (Fig. 17). The increase in activity by the addition of erythrose-4-phosphate has to be tested at again, since there is no report which shows an influence from erythrose-4-phosphate on the enzyme.

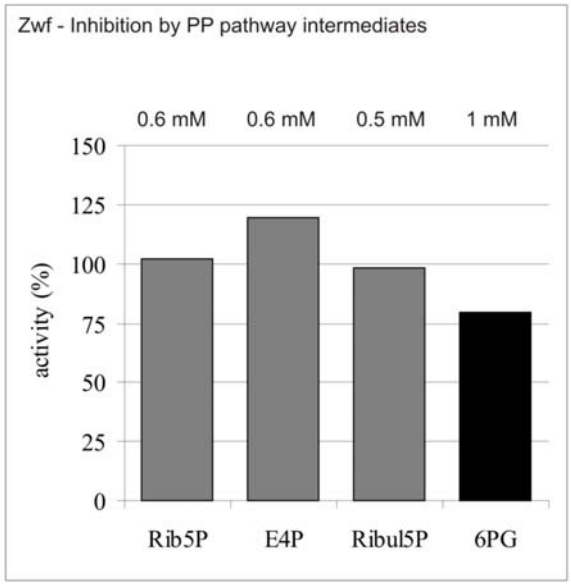

Figure 17: Inhibition screen of PP pathway intermediates. The glucose-6-phosphate concentration was kept at 300 µM. ribose-5-phosphate (Rib5P), erythrose-4-phosphate (E4P) and ribulose-5-phosphate (Ribul5P) do not indicate an inhibitory effect at concentrations, which are defined above the bars. The exception is 6-phosphogluconate (6PG), as the product, which was measured with a glucose-6-phosphate concentration of 0.5 mM.

ATP was tested in activity buffer with and without $MgCl_2$ as it forms complexes with Mg^{2+}. In both cases no effect was observed (Fig. 18). Using NADH as inhibitor resulted in highly fluctuating progressive curves and so only measurements with a stable progressive curve were evaluated (Fig. 18 & 19).

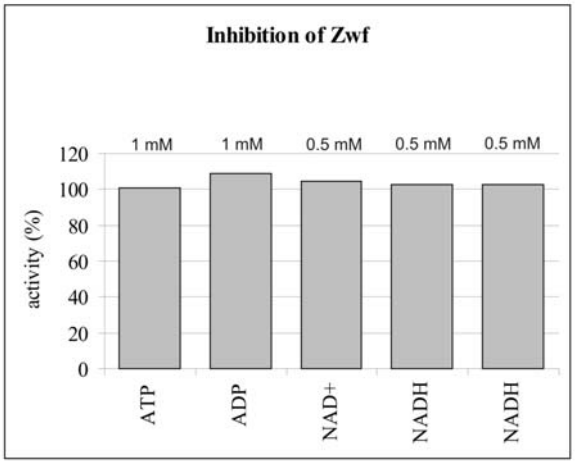

Figure 18: Zwf does not seem to be affected by ATP, ADP, NAD^+ or NADH at concentrations given above the bars. Glucose-6-phosphate concentration was kept 300 µM in the measurements of ATP and at 125 µM in the measurements with NAD^+ and NADH. The measurements with ADP and ATP were done without $MgCl_2$.

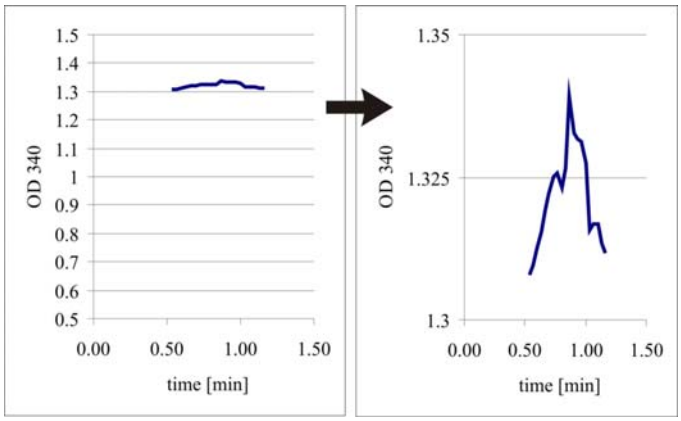

Figure 19: progressive curve with NADH as inhibitory compound. Some measurements have shown to highly fluctuate in a time course over 1.5 min. The effect can be seen, when the measurement is zoomed in what is illustrated on the right side of the figure.

The inhibitor-screen clearly shows that Zwf is not or only little influenced by metabolites other than NADPH, which will be further looked at in the next section. The only compounds which have shown an effect were 6-phosphogluconate and citrate at a glucose-6-phosphate concentration of 125 µM in the first measurements. For these compounds the glucose-6-phosphate concentration was set up to 300 µM in a second measurement, as it will better reflect the conditions in a cell. Only 6-phosphogluconate as the indirect product

of the reaction catalyzed had an effect on the performance of the enzyme and was further investigated in the following sections.

4.2.4 Determination of K_{iNADPH}

K_i-values of NADPH were determined with one substrate kept at a constant concentration, while the second substrate was varied at different constant inhibitor concentrations. According to the determined sequential ordered bi-bi-mechanism it was expected that NADPH will inhibit competitively in respect to $NADP^+$ and mixed non-competitive with respect to glucose-6-phosphate [5]. For NADPH as varied substrate, the glucose-6-phosphate concentration was held at 400 µM and $NADP^+$ was varied from 10 to 60 µM. As can be seen in Figure 20 A, the competitive inhibition was clearly seen in the double-reciprocal plot, since the straight lines have a common intercept on the Y-axis (1/V).

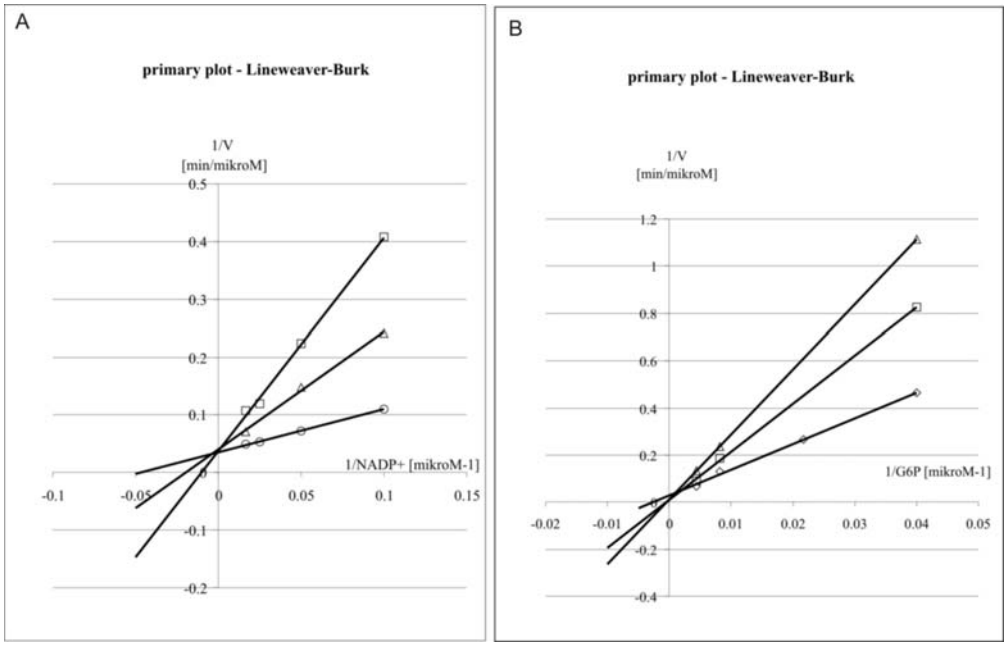

Figure 20: A: Lineweaver-Burk plot of competitive inhibition by NADPH with $NADP^+$ as the varied substrate: The different concentrations of inhibitor were □ = 150 µM Δ = 75 µM ○ = 0 µM . B: Lineweaver-Burk plot of mixed non-competitive inhibition by NADPH with G6P as the varied substrate. The different concentrations of inhibitor were: Δ = 150 µM □ = 75 µM ○ = 0 µM.

$K_{icNADP+}$ was determined to be 35µM. When glucose-6-phosphate was varied from 50 to 400 µM and $NADP^+$ was hold at 40 µM , the competive inhibition constant K_{icG6P} was determined to be 100 µM and the uncompetitive inhibition constant K_{iuG6P} was 455 µM (Fig 20 B). The inhibition constants were determined over secondary plots, where the the intercepts and slopes of the Lineweaver-Burk plots were plotted against the inhibitor

concentration. The determination of the uncompetitive inhibition was difficult, since the resolution of the ordinates was dissatisfactory.

4.2.5 Determination of K_{i6PG}

Since 6-phosphogluconate is the indirect product of the reaction catalyzed by Zwf and showed an effect in the inhibitor screen, the inhibition by this compound was further investigated. During the measurements with $NADP^+$ as the varied substrate, glucose-6-phosphate was added at a concentration of 0.3 mM. When glucose-6-phosphate was the varied substrate, $NADP^+$ was constantly added at 40 µM. The resulting Lineweaver-Burk plots are illustrated in Figure 27.

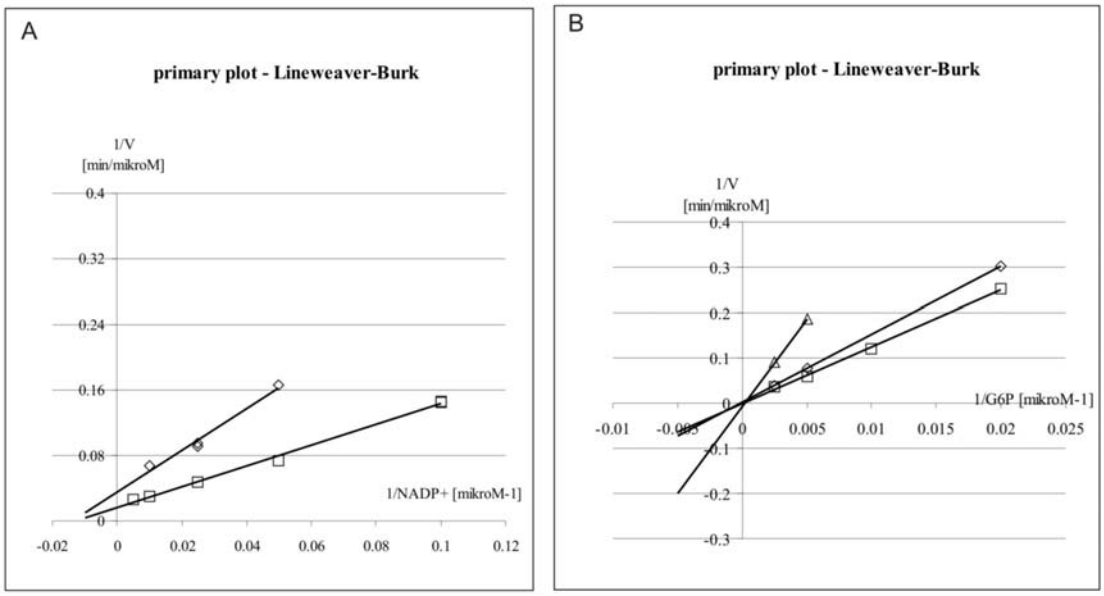

Figure 27: A: Lineweaver-Burk plot of 6-phosphogluconate inhibition with $NADP^+$ as the varied substrate: The different concentrations of inhibitor were ◊ = 5000 µM □ = 0 µM. B: Lineweaver-Burk plot of 6-phosphogluconate inhibition with G6P as the varied substrate. The different concentrations of inhibitor were: Δ = 5000 µM ◊ = 1000 µM □ = 0 µM.

The constants were determined by secondary plots. For $NADP^+$ the inhibition was non-competitive with a Kic_{NADP+} and a Kiu_{NADP+} of both 4.25 mM. The competitive inhibition constant in respect to glucose-6-phosphate was 2 mM.

4.3 Gnd

4.3.1 Purification of His_6-tagged Protein

Also Gnd, obtained from the ASKA library [32], was cultivated with 3 different concentrations of IPTG (0, 0.1 and 1 mM). As can be seen in Figure 15 A, the pellet from the centrifuged crude extract does not indicate an assembly of inclusion bodies. The enzyme was highly overexpressed with an IPTG concentration of 0.1 mM. Column operation worked well as the His_6-tagged enzyme was eluted at imidazole concentrations of 200 mM and more, without the detection of contaminants (Fig. 15 B).

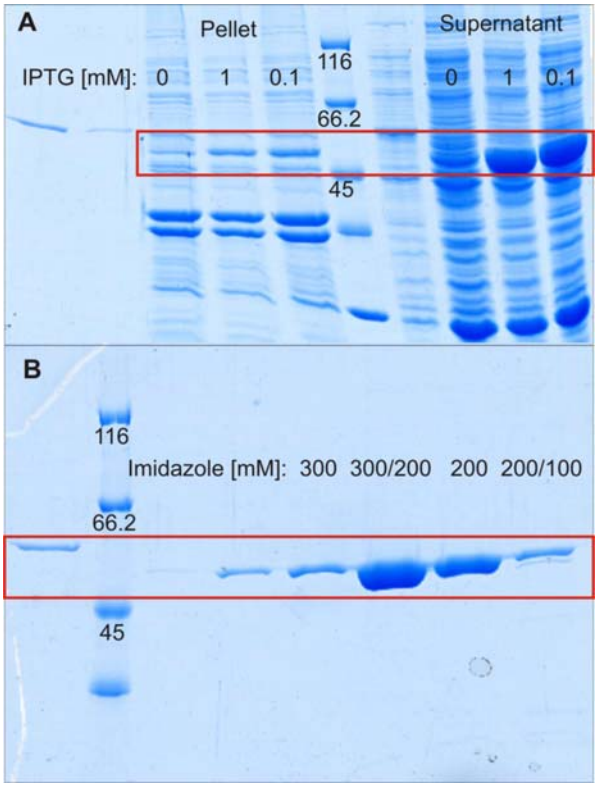

Figure 21: A: SDS gel after harvesting an overnight broth culture where overexpression was induced by three different concentrations of IPTG (0, 0.1 and 1 mM). As can be seen in the frame, induction by 1 and 0.1 mM IPTG led to excessive overexpression. The line in the middle shows the marker with bands at 116, 66.2 and 45 kDa. B: Elution profile after HisTrap operation. The enzyme could be eluted at imidazole concentrations of 200 mM (framed). High purity of the enzyme is indicated by the absence of other bands. On the left side the is the marker with bands at 116, 66.2 and 45 kDa.

Specific activity increased from 9600 Units/g to 54500 Units/g while the total enzyme concentration decreased from 3.77 mg/ml to 0.17 mg/ml as estimated with Biuret assay for the crude extract and Bradford assay for the dialysate (Fig. 16).

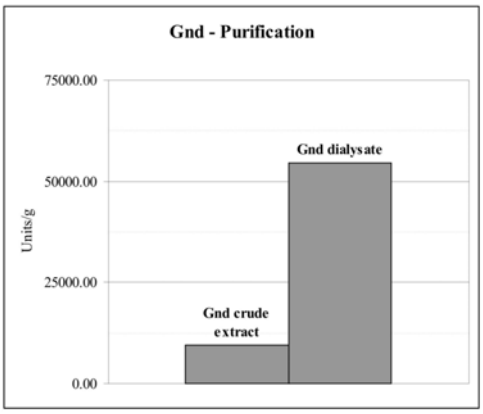

Figure 22: Purification of Gnd and evaluation of specific activity.

4.3.2 Determination of K_m

K_m values were determined with 20 µl of a 15 fold dilution of the dialysate in a total volume of 1 ml. 6-phosphogluconate concentrations were varied between 12.5 µM and 300 µM, while the $NADP^+$ concentrations covered a range from 7.5 µM to 60 µM. As shown in Figure 17 A, the measurements of initial velocities resulted in straight lines with a common point of intersection. From secondary plots the constants were determined. K_{mNADP+} was determined to be 9 µM, while the K_{m6PG} for 6-phosphogluconate was 19 µM. The dissociation constant of $NADP^+$ K_{iNADP+} had the value of 18.5 µM.

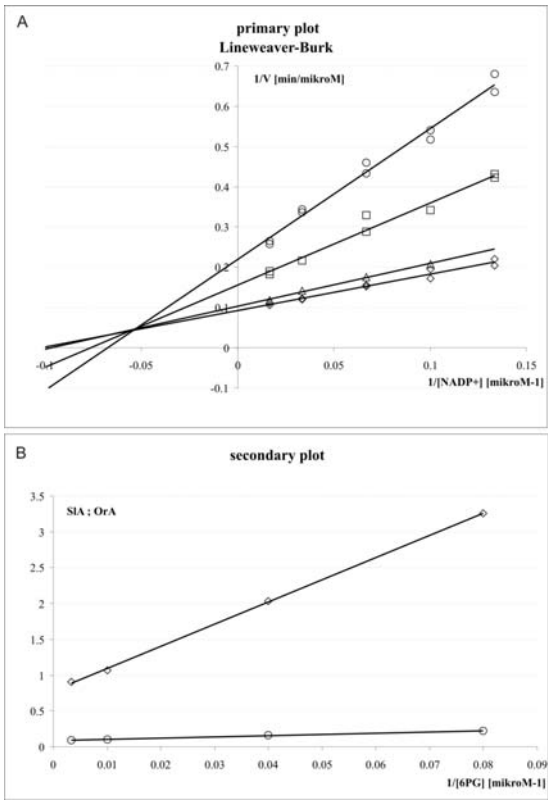

Figure 23: A: Lineweaver-Burk plot: The different concentrations of 6-phosphogluconate were ○ = 12.5 µM □ = 25 µM Δ = 100 µM ◊ = 300 µM . B: secondary plots: ○ = Or_A ◊ = Sl_A from the ordinate and abscissa of these plotes the constants can directly be determined.

4.3.3 Inhibitor screen

The inhibitor screen was done with 20 µl of 12 fold diluted enzyme. Substrate concentrations were chosen near the according K_m-values, so that inhibition would have been seen in a progressive curve and respectively in the resulting initial velocities. The concentrations of potential inhibitors were chosen to be close to physiological values ([35], supplement 2) and stocks were done in assay buffer or water and stored at -20°C. The potential inhibitors were thawed on ice and tested for no influence on the pH not more than 0.1 pH units. Especially in organic acids like citrate and oxaloacetate the pH had to be adjusted with 5 M KOH and 6 M HCl. Additionally, the behaviour of the enzyme in 100 mM Tris HCl and 10 mM $MgCl_2$ was tested in a pH range from 6.7 to 7.7 units. It does not seem like the pH does influence the acitivity of the enzyme in a range from 7.3 to 7.6 pH units (Fig. 24) and since the different samples did only show a pH variability within that range, a potential effect of pH can be neglected.

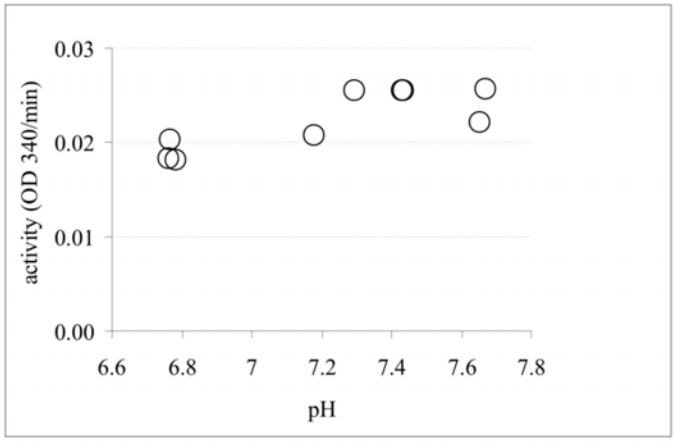

Figure 24: The dependency of Zwf activity from pH in a range of 6.8 to 7.6. The activity is nearly constant in the range of 7.3 to 7.5 pH units.

In contrast to Zwf, Gnd was highly affected by intermediates of glycolysis. From the glycolytic compounds only fructose-1,6-bisphosphate even showed an impact on the activity of Gnd at 6-phosphogluconate concentrations of 5 mM (Fig. 24 B).

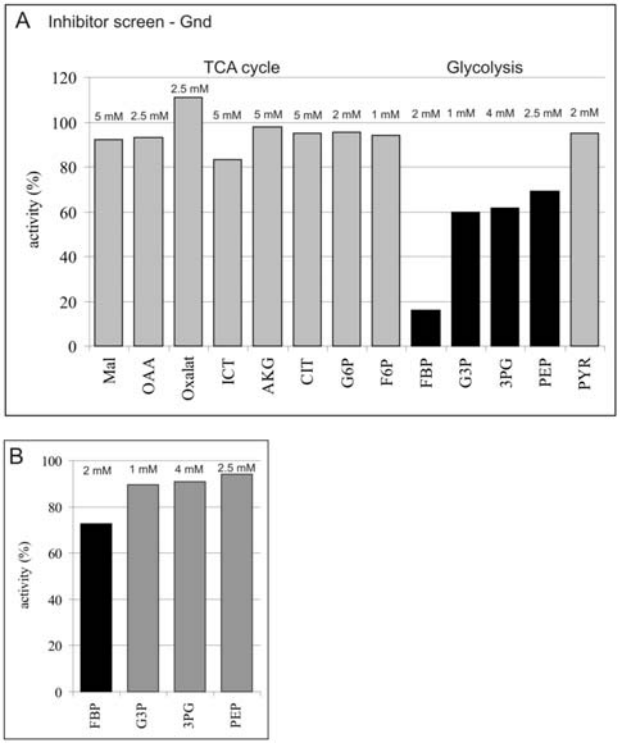

Figure 24: A: Inhibitor screen from intermediates of TCA cycle and glycolysis. [NADP+] was 20 µM and [6PG] 40 µM. The values above the bars indicate the chosen inhibitor concentration. B: When 6PG was raised to 5 mM, only Fructose-1,6-bisphosphate had an effect

The compounds tested from PP pathway have shown to inhibit Gnd (Fig 25). Especially the effect of ribulose-5-phosphate as the product was striking. With 6-phosphogluconate concentrations of 5 mM the effect was not present anymore.

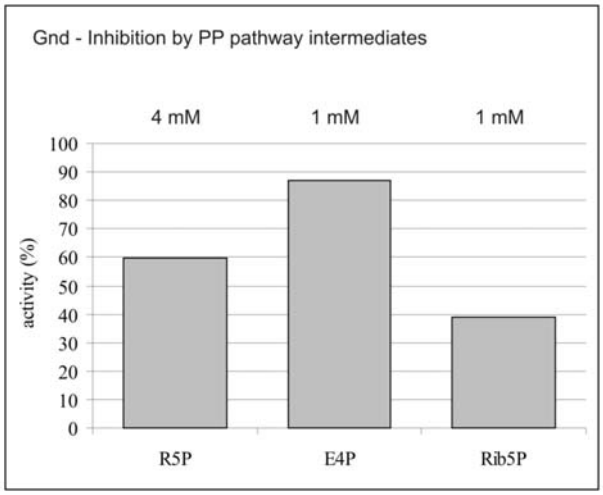

Figure 25: Inhibition of Intermediates of the PP pathway at 6-phosphogluconate concentrations of 60 µM and NADP+ concentrations of 30 µM. The concentrations of the intermediates is given above the bars.

ATP was tested in activity buffer with and without $MgCl_2$ as it formes complexes with Mg^{2+}. In the case when $MgCl_2$ was present in the buffer at a concentration of 10 mM, no impact on the enzyme's activity could be observed. Without $MgCl_2$, 1 mM ATP reduced the activity to 60 %. With concentrations of 6-phosphogluconate as high as 0.5 mM, no effect was present anymore.

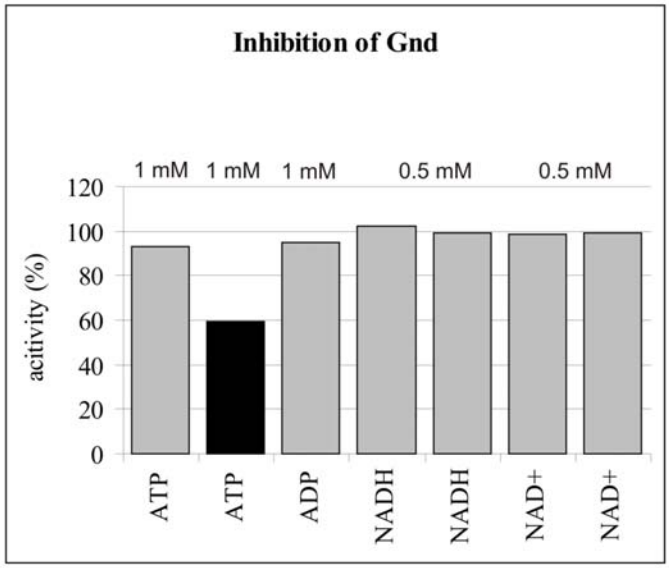

Figure 26: Inhibtion of Gnd by ATP, ADP , NAD^+ and NADH. The numbers above the bars give the concentration of the corresponding compound. The bar on the left side was done with 0.5 mM 6-phosphogluconate, whereas in the other measurements 40 to 60 µM 6-phosphogluconate was used. $NADP^+$ concentrations were 20 to 30 µM.

As mentioned above, the NADH measurements caused some problems with fluctuating progressive curves.

4.3.4 Determination of inhibition by NADPH

To define the impact of NADPH on Gnd, both substrates were varied with a constant concentration of the second substrate. During one series of measurements the inhibitor concentration was kept constant. 6-phosphogluconate was held at 300 µM, while $NADP^+$ was varied from 7.5 µM to 60 µM.

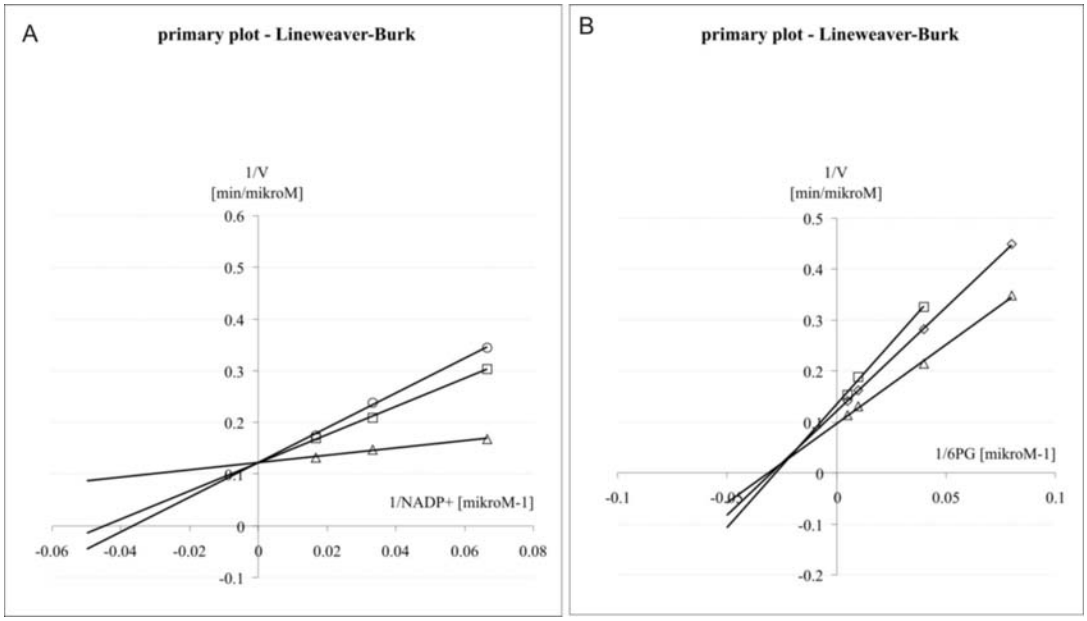

Figure 27: A: Lineweaver-Burk plot of NADPH inhibition with $NADP^+$ as the varied substrate: The different concentrations of inhibitor were ○ = 75 µM □ = 50 µM Δ = 0 µM . B: Lineweaver-Burk plot of NADPH inhibition with G6P as the varied substrate. The different concentrations of inhibitor were: Δ = 75 µM ○ = 50 µM □ = 0 µM.

The double-reciprocal plot clearly shows that Gnd is competitively inhibited by NADPH with respect to $NADP^+$ with a $K_{icNADP+}$ of 20 µM (Fig. 27 A). When 6-phosphogluconate was varied from 12.5 µM to 200 µM, $NADP^+$ was held at 200 µM. The resulting double-reciprocal plot shows a mixed non-competitive type of inhibition with a Kic_{6PG} of 130 µM and Kiu_{6PG} of 190 µM (Fig. 27 B).

4.3.5 Determination of inhibition by ribulose-5-phosphate

As Ribulose-5-phosphate is the second product of the reaction catalyzed by Gnd, K_i values were determined. The Lineweaver-Burk plots show that ribulose-5-phosphate inhibits Gnd competitively with respect to 6-phosphogluconate and mixed non-competitive with respect to $NADP^+$ (Fig. 27). To determine the inhibition constants, $NADP^+$ was varied from 10 to 200 µM, while 6PG was kept constant at a concentration of 100 µM and the inhibitor

concentrations were hold at 0 and 500 µM during one series of measurements. When 6PG was the varied substrate (20 – 500 µM) $NADP^+$ was kept at 50 µM.

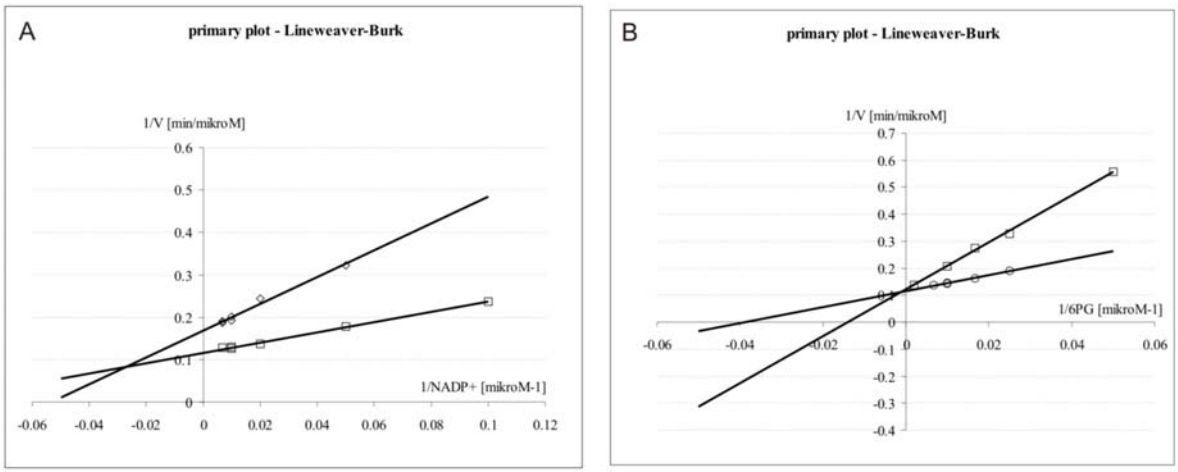

Figure 27: A: Lineweaver-Burk plot of Ribulose-5-phosphate inhibition with $NADP^+$ as the varied substrate: The different concentrations of inhibitor were ◊ = 500 µM □ = 0 µM. B: Lineweaver-Burk plot of Ribulose-5-phosphate inhibition with G6P as the varied substrate. The different concentrations of inhibitor were: □ = 500 µM ○ = 0 µM.

The constants were determined by secondary plots. For $NADP^+$ the inhibition was mixed non-competitive with a $K_{icNADP+}$ of 311 µM and a $K_{iuNADP+}$ of 1.16 mM. The competitive inhibition with respect to 6-phosphogluconate was 250 µM.

4.4 Application of determined parameters

As the different kinetic parameters of Gnd and Zwf were determined, the impact of different NADPH/$NADP^+$-ratios was further explored, based on a total NADP(H) concentration of 100 µM [internal communication]. Equation 13 was used simulate what for different ratios of NADPH to $NADP^+$ in a excel program. The used parameters are given in table 6 and the results are shown in figure 28.

	Zwf		Gnd	
Inhibitor: NADPH	K_{ic}	K_{iu}	K_{ic}	K_{iu}
$NADP^+$	35 µM	-	20 µM	-
glucose-6-phosphate	100 µM	455 µM	-	-
6-phosphogluconate	-	-	130 µM	190 µM
Inhibitor: 6-phospho gluconate and ribulose-5-phosphate, respectively	K_{ic}	K_{iu}	K_{ic}	K_{iu}
$NADP^+$	4250 µM	4250 µM	311 µM	1160 µM
glucose-6-phosphate	2000 µM	-	-	-
6-phosphogluconate	-	-	250 µM	-
	K_m	K_{iNADP^+}	K_m	K_{iNADP^+}
$NADP^+$	23 µM	90 µM	9 µM	18.5 µM
glucose-6-phosphate	136 µM	-	-	-
6-phosphogluconate	-	-	19 µM	-

Table 6: Summary of determined parameters for Gnd and Zwf with respect to $NADP^+$ and NADPH.

The results clearly show, that the ratio of $NADP^+$ to NADPH has high impact on the enzymes activity because if the ratio was increased from 0.5 to 1 the activity of the enzyme was almost doubled (Fig. 28).

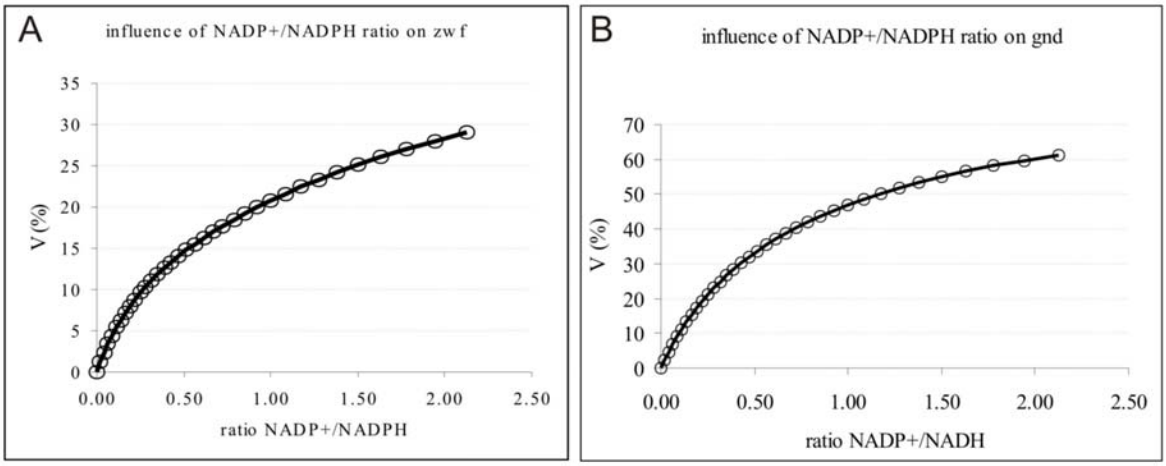

Figure 28: influence of the $NADP^+$/NADPH ratio on the action of Zwf (A) and Gnd (B). On the X-axis the ratio is given and on the Y-axis the percentage of V is given.

Next the influence of substrate availability was tested on both enzymes, with equation 5. 6-phosphogluconate was varied from 0.2 to 2 mM and glucose-6-phosphate from 0.2 to 4 mM. $NADP^+$ concentrations were kept constant at 0.05 mM. The results in Figure 29 show that Gnd is only little influenced by various substrate concentrations, while Zwf shows high dependency on substrate availability at concentrations between 0.2 and 2 mM.

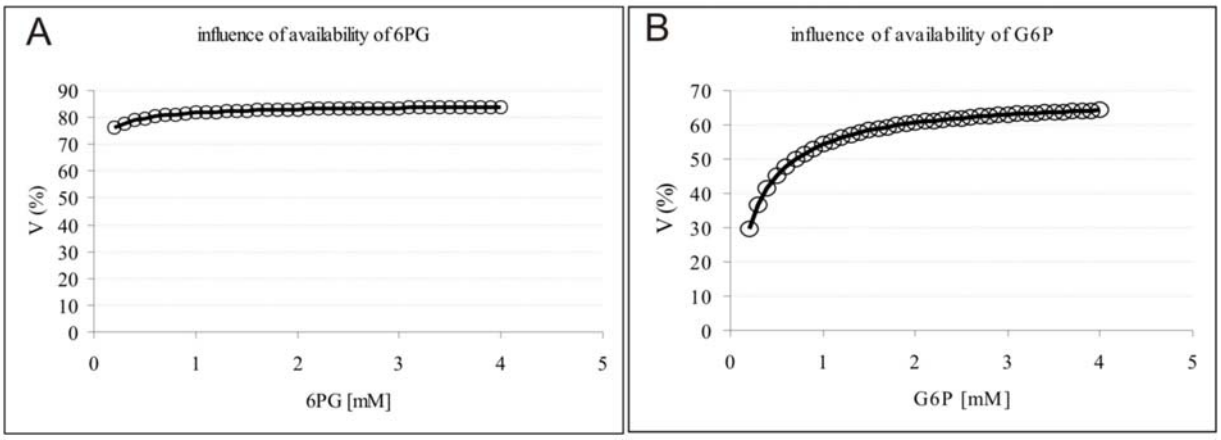

Figure 29: A: Dependency of Gnd on various substrate concentrations; B: Dependency of Zwf on various substrate concentrations.

Additionally, product inhibition of the enzymes by 6-phosphogluconate and ribulose-5-phosphate was analysed (Fig. 30). Therefore the concentration of $NADP^+$ was held constant at 0.05 mM and the particular second substrate was kept at 1 mM. For ribulose-5-phosphate concentrations ranging from 0.01 to 1 mM were analyzed. For 6-phosphogluconate concentrations from 0.2 to 2 mM were considered. For each enzyme equation 13 was used for analysis

.

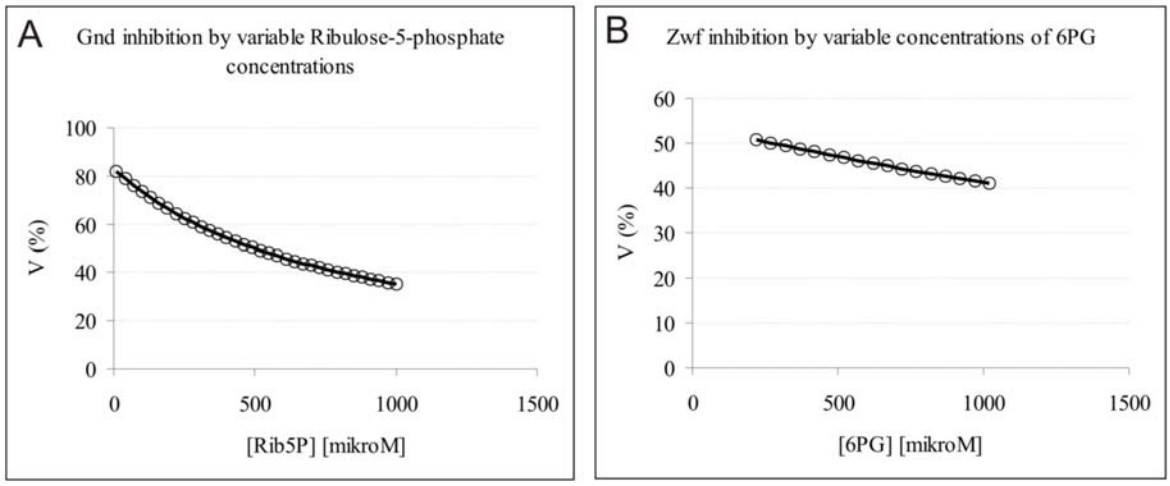

Figure 30: A: Inhibition of Gnd by ribulose-5-phosphate; B: Inhibition of Zwf by 6-phosphogluconate

The results show that the activity of Gnd is highly dependent on product concentrations, since in the considered range of concentration the activity falls down to half of its value. In contrast 6-phosphogluconate does not exhibit a big effect on the action of Zwf, as there is only a decrease of 10% in velocity in the considered range of concentration.

5 Discussion and Outlook

5.1 Zwf and Gnd

The overexpression of the His_6-tagged proteins and the following purification via HisTrap was straight-forward with active and pure protein. For the kinetic characterization , two buffers were tested, the 100 mM Tris-HCl , 10 mM $MgCl_2$ buffer was chosen, since $MgCl_2$ is reported to enhance Zwf activity [9]. It was important to test, if the strength of the buffer can be increased, since organic acids led to pH change. It would be preferable if no treatment of the compounds has to be done with respect to pH, since this will affect the exact concentrations of these compounds. This is especially critical when small concentrations have to be used. Problems with NADH and NADPH measurements due to fluctuation were avoided by good mixing before the measurement and setting a new reference at 340 nm. This seemed to be sufficient for measurements of these compounds and no further improvement had to be done. Since most of the compounds are not very stable at room temperature stock solutions had to be thawed on ice and to prevent temperature changes only small volumes could be pipetted to a certain sample. For the primary screen substrate concentrations were chosen near the K_m values to detect the inhibitory effects exhibited by metabolites. In secondary measurements the substrate concentrations were raised to identify the strong inhibitors. For determination of kinetic constants double-reciprocal and secondary plots were used. Since this manual analysis potentially yields errors, fitting direct plots, where the initial velocities are plotted against initial substrate concentrations, by mathematical software (Kaleidagraph or Scientist) has to be evaluated as an alternative.

The screen over a range of 20 metabolites has shown that the activity of Zwf is only influenced by 6-phosphogluconate and NADPH. Reported effects of Glyceraldehyde-3-phosphate and NADH were not detected at concentrations of 1 mM and 0.5 mM, respectively [9]. Whereas the inhibition constants for 6-phosphogluconate were very high, the K_{ic}-value of the inhibition by NADPH was very low (35 μM), as well as the K_m-values for $NADP^+$ (23 μM). The noncompetitive inhibition by NADPH with respect to glucose-6-phosphate was not comparable to the one observed by Sanwal and the inhibition constants were determined to be a 3-fold higher (Table 2) [9]. However, the results clearly indicate that the branchpoint between glycolysis and PP pathway is mainly regulated by the $NADP^+$ to NADPH ratio as it is already reported for other organisms [10]. To further support this,

the kinetic parameters determined were used to investigate the influence of the $NADP^+$/NADPH ratio on the velocity of the Zwf reaction. The simulations clearly show a dependency of the enzymes activity on the cofactor ratio, but Zwf also seems to be regulated by substrate availability. For further investigation of the dependency of Zwf on its substrate and on the cofactor ratio exact *in vivo* concentrations of these compounds have to be determined. If the glucose-6-phosphate concentration is relatively high with respect to the determined K_m value under several conditions, the effect of substrate availability will not be present. This will lead to the implication that the $NADP^+$/NADPH ratio is rather stable under several conditions and defines the flux into PP pathway, which is observed to be robust [20]. To neglect potential genetic regulation mRNA levels of Zwf have to be measured under several conditions.

In contrast to Zwf, the action of Gnd seems to be affected by several compounds from glycolysis, compounds directly downstream in the PP pathway and also by ATP, as it showed an inhibitory effect when measured without $MgCl_2$. A second compound which highly influenced the activity of Gnd was fructose-1,6-bisphosphate. The *in vivo* inhibitory effect by these compounds has to be further investigated, as metabolite concentrations can be determined. In the present thesis it was mainly focussed on the inhibition by NADPH and ribulose-5-phosphate, which exhibited high impact on the performance of the enzyme, as they are the products of Gnd reaction. The measured competitive inhibition constants were 20 µM and 250 µM, respectively. The action of Gnd does not highly depend on 6-phosphogluconate availability, as the K_m value is very low (19µM), which lies within the reported range (Table 3) [27]. The use of the determined kinetic parameters in simulations reveals that Gnd is highly regulated by its products ribulose-5-phosphate and NADPH. Especially in the case of Gnd it is of high value to know exact *in vivo* metabolite concentrations to gain more insights into its regulation by other compounds than NADPH and ribulose-5-phosphate.

In summary the NADPH/$NADP^+$ ratio seems to be an important but not the only regulator of PP pathway. The ratio is highly involved in the regulation of both enzymes, which reside at the branch point of PP pathway and Glycolysis. Further studies have to be done to reveal the impact of regulation by compounds other than NADPH and $NADP^+$.

5.2 UdhA

UdhA was overexpressed with an N-terminal His_6-tag. In general this is a straight forward method for protein purification, that is fast and yields high purity. However in our case

inclusion bodies had formed and protein renaturation was necessary. Since on- column-refolding failed because of the multimeric form of the enzyme and rapid dilution yielded no activity in the tested samples, it indicates that probably the N-terminus is directly involved in the correct folding of the protein. Additionally we attempted to overexpress native UdhA for purification with an affinity column, which would retain all proteins that react with a cofactor. However, the insertion of the *udhA* gene into various vectors failed repeatedly for unknown reasons, although a positive controls such as cloning the previous used DNA fragment into pBlueskriptII SK(+) worked. One potential problem might be our choice of an overhang of just two basepairs at each end of the recognition sites, so that the restriction would be hindered. According to NEB catalogue this will work, but they recommend 4-6 basepairs between the blunt end of the fragment and the recognition site for restriction. The best way to go would be the use of new primers, which will give a longer overhang from the recognition site to the blunt end of the fragment.

Generally, kinetic characterization of UdhA has to be done, since the impact of this enzyme and its potential reversibility under aerobic batch conditions on glucose is unclear. Kinetic studies will reveal how the enzyme is allosterically regulated, as well as by cofactors. Additionally this will reveal if a certain cofactor ratio is maintained in a cell under several conditions or at least in which range the cofactor ratio can change. The resulting impact of the cofactor ratio on the regulation of metabolism has to be examined.

5.3 Dynamic modelling

Dynamic modelling has the potential of resolving the regulation of metabolism. *In vitro* experiments will reveal the impact of a particular compound on the performance of an enzyme. In combination with exact *in vivo* concentrations of metabolites the regulation of enzymes involved in branching reactions can be qualitatively considered. That makes dynamic modelling to a powerful tool in answering specific biological questions. A problem is that the information will only be qualitative, since assay conditions do not resemble in vivo conditions.

Dynamic modelling of whole systems will be valuable in simulating the response of metabolism with respect to different conditions. However, up to date there is a lack of kinetic information, what sets clear constraints to dynamic models [5]. Further investigation has to be done, to achieve dynamic models which highly reflect in vivo conditions and their dynamic behaviour.

6 Acknowledgements

I thank Uwe Sauer for giving me the opportunity of carrying out my diploma thesis in his lab, for his scientific support and for critically reading this script.

Special thanks to:

Tobias Fuhrer for excellent supervision.

Sauer group for having a really good time.

Claudio Guetg and Philipp Lienemann.

Prof. Dr. Rudi Glockshuber and members of the Aebersold group for answering questions.

References

1. Fuhrer, T. and U. Sauer, *Microbial NADPH metabolism.* in preparation, 2006.
2. Brumaghim, J.L., et al., *Effects of hydrogen peroxide upon nicotinamide nucleotide metabolism in Escherichia coli: changes in enzyme levels and nicotinamide nucleotide pools and studies of the oxidation of NAD(P)H by Fe(III).* J Biol Chem, 2003. **278**(43): p. 42495-504.
3. Greenberg, J.T., et al., *Activation of oxidative stress genes by mutations at the soxQ/cfxB/marA locus of Escherichia coli.* J Bacteriol, 1991. **173**(14): p. 4433-9.
4. Harold, F., *The Vital Force: A Study of Bioenergetics*. 1986, New York: Freeman and Company.
5. Chassagnole, C., et al., *Dynamic modeling of the central carbon metabolism of Escherichia coli.* Biotechnology and Bioengineering, 2002. **79**(1): p. 53-73.
6. Orthner, C.L. and L.I. Pizer, *An evaluation of regulation of the hexose monophosphate shunt in Escherichia coli.* J Biol Chem, 1974. **249**(12): p. 3750-5.
7. Sauer, U., et al., *The soluble and membrane-bound transhydrogenases UdhA and PntAB have divergent functions in NADPH metabolism of Escherichia coli.* Journal of Biological Chemistry, 2004. **279**(8): p. 6613-6619.
8. Dyson, J.E. and R.E. D'Orazio, *Sheep liver 6-phosphogluconate dehydrogenase. Inhibition by nucleoside phosphates and by other metabolic intermediates.* J Biol Chem, 1973. **248**(15): p. 5428-35.
9. Sanwal, B.D., *Regulatory Mechanisms Involving Nicotinamide Adenine Nucleotides as Allosteric Effectors .3. Control of Glucose 6-Phosphate Dehydrogenase.* Journal of Biological Chemistry, 1970. **245**(7): p. 1626-&.
10. Moritz, B., et al., *Kinetic properties of the glucose-6-phosphate and 6-phosphogluconate dehydrogenases from Corynebacterium glutamicum and their application for predicting pentose phosphate pathway flux in vivo.* Eur J Biochem, 2000. **267**(12): p. 3442-52.
11. Hoek, J.B. and J. Rydstrom, *Physiological Roles of Nicotinamide Nucleotide Transhydrogenase.* Biochemical Journal, 1988. **254**(1): p. 1-10.
12. Bizouarn, T., et al., *The organization of the membrane domain and its interaction with the NADP(H)-binding site in proton-translocating transhydrogenase from E. coli.* Biochim Biophys Acta, 2002. **1555**(1-3): p. 122-7.
13. Zerez, C.R., et al., *Negative Modulation of Escherichia-Coli Nad Kinase by Nadph and Nadh.* Journal of Bacteriology, 1987. **169**(1): p. 184-188.
14. Canonaco, F., et al., *Metabolic flux response to phosphoglucose isomerase knock-out in Escherichia coli and impact of overexpression of the soluble transhydrogenase UdhA.* Fems Microbiology Letters, 2001. **204**(2): p. 247-252.
15. Emmerling, M., et al., *Metabolic flux responses to pyruvate kinase knockout in Escherichia coli.* J Bacteriol, 2002. **184**(1): p. 152-64.
16. Boonstra, B., et al., *The udhA gene of Escherichia coli encodes a soluble pyridine nucleotide transhydrogenase.* J Bacteriol, 1999. **181**(3): p. 1030-4.
17. Boonstra, B., et al., *Cofactor regeneration by a soluble pyridine nucleotide transhydrogenase for biological production of hydromorphone.* Appl Environ Microbiol, 2000. **66**(12): p. 5161-6.
18. Wood, T., *Physiological Functions of the Pentose-Phosphate Pathway.* Cell Biochemistry and Function, 1986. **4**(4): p. 241-247.
19. Fuhrer, T., E. Fischer, and U. Sauer, *Experimental identification and quantification of glucose metabolism in seven bacterial species*, in *J Bacteriol*. 2005. p. 1581-90.

20. Perrenoud, A. and U. Sauer, *Impact of global transcriptional regulation by ArcA, ArcB, Cra, Crp, Cya, Fnr, and Mlc on glucose catabolism in Escherichia coli.* Journal of Bacteriology, 2005. **187**(9): p. 3171-3179.
21. Banerjee, S. and D.G. Fraenkel, *Glucose-6-Phosphate Dehydrogenase from Escherichia-Coli and from a High-Level Mutant.* Journal of Bacteriology, 1972. **110**(1): p. 155-&.
22. Cavalier.Rl and H.Z. Sable, *Enzymes of Pentose Biosynthesis .2. Evidence That Proposed Control of Glucose-6-Phosphate Dehydrogenase by Reduced Diphosphopyridine Nucleotide Is an Instrumental Artifact.* Journal of Biological Chemistry, 1973. **248**(8): p. 2815-2817.
23. Rowley, D.L., A.J. Pease, and R.E. Wolf, *Genetic and Physical Analyses of the Growth Rate-Dependent Regulation of Escherichia-Coli Zwf Expression.* Journal of Bacteriology, 1991. **173**(15): p. 4660-4667.
24. Giro, M., N. Carrillo, and A.R. Krapp, *Glucose-6-phosphate dehydrogenase and ferredoxin-NADP(H) reductase contribute to damage repair during the soxRS response of Escherichia coli.* Microbiology, 2006. **152**(Pt 4): p. 1119-28.
25. *BRENDA - The comprehensive enzyme information system*, Prof. Dr. D. Schomburg, Institut fuer Biochemie, Universität zu Köln.
26. Rippa, M., et al., *6-phosphogluconate dehydrogenase: the mechanism of action investigated by a comparison of the enzyme from different species.* Biochimica Et Biophysica Acta-Protein Structure and Molecular Enzymology, 1998. **1429**(1): p. 83-92.
27. de Silva, A.O. and D.G. Fraenkel, *The 6-phosphogluconate dehydrogenase reaction in Escherichia coli.* J Biol Chem, 1979. **254**(20): p. 10237-42.
28. Francesco M. Veronese, E.B., and Angelo Fontana, *Isolation and Properties of 6-Phosphogluconate Dehydrogenase from Escherichia coli. some Comparisons with the Thermophilic Enzyme from Bacillus stearothermophilus.* Biochemistry, 1976. **15**.
29. Berg, J.M., J.L. Tymoczko, and L. Stryer, *Biochemistry*. 5 ed. 2002, New York: W. H. Freeman and Co.
30. Bisswanger, P.D.H., *Enzyme Kinetics : Principles and Methods*. 2002, Wiley-VCH Verlag GmbH.
31. *Enzyme inhibition*, Faculty of Engineering, Science and the Built Environment.
32. Kitagawa, M., et al., *Complete set of ORF clones of Escherichia coli ASKA library (A Complete Set of E. coli K-12 ORF Archive): Unique Resources for Biological Research*, in *DNA Res*. 2005. p. 291-9.
33. Sambrook, J. and D.W. Russel, *Molecular Cloning : a laboratory manual*. 3 ed, ed. C.S.H.L. Press. 2001, Cold Spring Harbor, New York: Cold Spring Harbor Laboratory Press.
34. *Current Protocols in Protein Science*, Wiley.
35. Kümmel, A., S. Panke, and M. Heinemann, *Putative regulatory sites unraveled by network-embedded thermodynamic analysis of metabolome data.* EMBO and Nature Publishing Group, 2006.